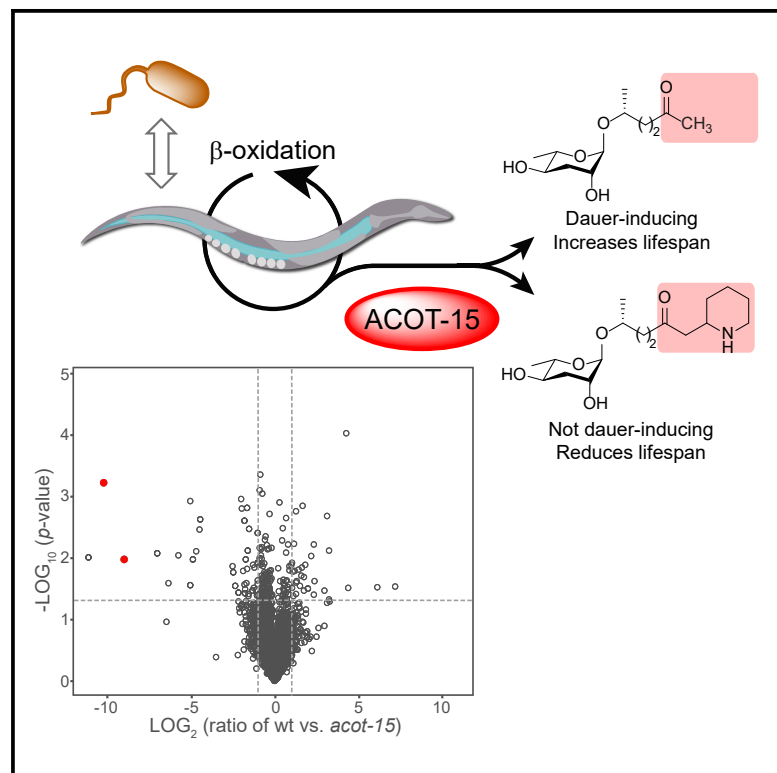


Cell Chemical Biology

An acyl-CoA thioesterase is essential for the biosynthesis of a key dauer pheromone in *C. elegans*

Graphical abstract



Authors

Subhradeep Bhar, Chi-Su Yoon, Kevin Mai, ..., Laura S. Bailey, Kari B. Basso, Rebecca A. Butcher

Correspondence

butcher@chem.ufl.edu

In brief

Bhar et al. identify an acyl-CoA thioesterase, ACOT-15, that terminates the β -oxidation pathway in pheromone biosynthesis in *C. elegans* and produces a key methyl ketone ascaroside that induces dauer, as well as a non-dauer-inducing piperidyl ascaroside. Bacterial food impacts the amount of the piperidyl ascaroside made by the worm.

Highlights

- The acyl-CoA thioesterase ACOT-15 biosynthesizes key ascaroside pheromones in worms
- ACOT-15 terminates β -oxidation, producing a dauer-inducing methyl ketone ascaroside
- ACOT-15 also generates a non-dauer-inducing piperidyl ascaroside
- Bacterial food affects the production of the piperidyl ascaroside by the worm



Article

An acyl-CoA thioesterase is essential for the biosynthesis of a key dauer pheromone in *C. elegans*

Subhradeep Bhar,^{1,2} Chi-Su Yoon,^{1,2} Kevin Mai,¹ Jungsoo Han,¹ Dilip V. Prajapati,¹ Yuting Wang,¹ Candy L. Steffen,¹ Laura S. Bailey,¹ Kari B. Basso,¹ and Rebecca A. Butcher^{1,3,*}

¹Department of Chemistry, University of Florida, Gainesville, FL 32611, USA

²These authors contributed equally

³Lead contact

*Correspondence: butcher@chem.ufl.edu

<https://doi.org/10.1016/j.chembiol.2023.12.006>

SUMMARY

Methyl ketone (MK)-ascarosides represent essential components of several pheromones in *Caenorhabditis elegans*, including the dauer pheromone, which triggers the stress-resistant dauer larval stage, and the male-attracting sex pheromone. Here, we identify an acyl-CoA thioesterase, ACOT-15, that is required for the biosynthesis of MK-ascarosides. We propose a model in which ACOT-15 hydrolyzes the β -keto acyl-CoA side chain of an ascaroside intermediate during β -oxidation, leading to decarboxylation and formation of the MK. Using comparative metabolomics, we identify additional ACOT-15-dependent metabolites, including an unusual piperidyl-modified ascaroside, reminiscent of the alkaloid pelletierine. The β -keto acid generated by ACOT-15 likely couples to 1-piperidine to produce the piperidyl ascaroside, which is much less dauer-inducing than the dauer pheromone, asc-C6-MK (ascr#2, 1). The bacterial food provided influences production of the piperidyl ascaroside by the worm. Our work shows how the biosynthesis of MK- and piperidyl ascarosides intersect and how bacterial food may impact chemical signaling in the worm.

INTRODUCTION

The nematode *C. elegans* secretes the ascarosides as signaling molecules to communicate with other nematodes and to modify its development and behavior in response to changing environmental conditions.^{1–9} The ascarosides are structurally diverse derivatives of the 3,6-dideoxy-L-sugar ascarylose that have fatty acid-derived side chains. The activities of the ascarosides are dictated by nuances in their chemical structures, including the length of their side chain, the position at which the side chain is attached to the ascarylose sugar, the presence or absence of α,β -unsaturation, and the presence or absence of various modifications on the ascarylose sugar (head groups) or on the side chain terminus (terminus groups) (Figure 1A). The ascarosides work as mixtures, and their activities are concentration-dependent.^{2–4} For example, when faced with adverse environmental conditions, including high population density, low food availability, and high temperatures, *C. elegans* uses a mixture of ascarosides known as the dauer pheromone to induce development of a stress-resistant larval stage, known as the dauer.^{1–3,5,11} Of the dauer pheromones in *C. elegans*, one of the most potent is an ascaroside with a side chain that terminates in a methyl ketone (MK), asc-C6-MK (1) (Figure 1A).¹ At mid- to high-nanomolar concentrations, this pheromone induces dauer and repulses hermaphrodites, but at picomolar/low nanomolar

concentrations, it attracts males as part of a hermaphrodite-produced sex pheromone and suppresses foraging.^{1,4,9} This pheromone has been identified in a diversity of other *Caenorhabditis* species besides *C. elegans* and functions as the main dauer pheromone in *Caenorhabditis briggsae*.^{12,13} As the vast majority of ascarosides that have been identified have a fatty-acid side chain that terminates in a carboxylic acid or a modified carboxylic acid, asc-C6-MK (1), along with the glycosylated derivative glc-asc-C6-MK (2), have structurally unusual side chains (Figure 1A).^{1,4}

The ascaroside pheromones are biosynthesized from long-chain ascarosides that have their side chains shortened through peroxisomal β -oxidation (Figure 1B).^{14–20} Each round of β -oxidation, which shortens the side chains by two carbons, involves four enzymes, an acyl-CoA oxidase (ACOX), an enoyl-CoA hydratase (MAOC-1), a (3*R*)-hydroxyacyl-CoA dehydrogenase (DHS-28), and a 3-ketoacyl-CoA thiolase (DAF-22).^{14,16,17} The five ACOX enzymes that have been shown to participate in ascaroside biosynthesis have different side-chain length preferences, and the expression levels of these enzymes have been shown to influence the side-chain lengths of the ascaroside pheromones that are produced.^{18–20} Ultimately, the β -oxidation process must be terminated to yield ascaroside pheromones with defined side-chain lengths. In yeast, plants, and mammals, the process of fatty acid β -oxidation can be terminated through



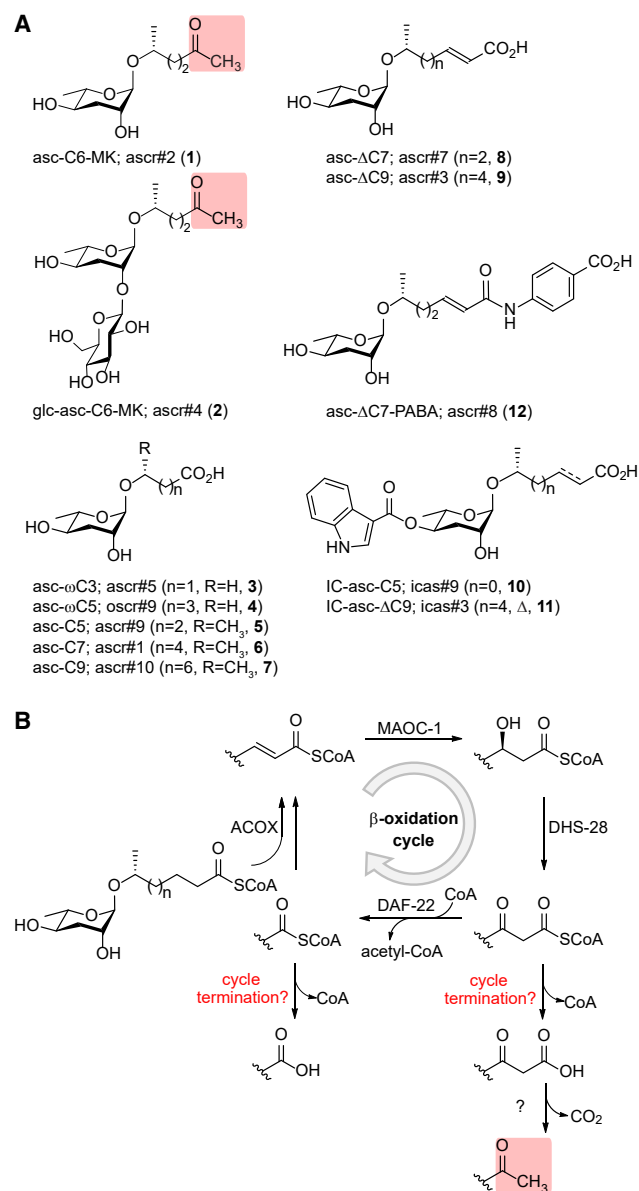


Figure 1. Structures of some ascarosides, the role of β -oxidation in ascaroside biosynthesis, and candidate mechanisms for β -oxidation termination

(A) The chemical structures of some abundant ascarosides in the *C. elegans* exometabolome. These ascarosides include the MK-containing ascarosides, asc-C6-MK (1) and glc-asc-C6-MK (2). The nomenclature used in this study for the ascarosides is based on their modular structure: head group-asc-(ω)(Δ)C#-terminus group, where C# refers to the number of carbons in the side chain.¹⁰ (B) Ascaroside pheromones are synthesized from long-chain ascarosides which have their side chains shortened through β -oxidation. The mechanisms used to terminate the β -oxidation process and generate side chains terminating in either carboxylic acids or methyl ketones have not been identified. A candidate mechanism for MK biosynthesis is shown.

hydrolysis of the fatty acyl-CoAs by a family of acyl-CoA thioesterase (ACOT) enzymes that have different substrate preferences.²¹ ACOT-1 in *C. elegans* was implicated in the biosynthesis of ascarosides with 8–13 carbon side chains, since a

acot-1 mutant strain produces reduced amounts of these ascarosides.²²

The biosynthetic steps leading to the MK moiety in *C. elegans* have not been studied. Methyl ketones are present in many natural products, most notably volatile plant compounds, such as 2-tridecanone and 2-undecanone, that are produced as deterrents against herbivorous insects.^{23,24} The biosynthesis of these compounds is best characterized in tomato, where the MK moiety is derived from intermediates in fatty acid biosynthesis.²⁵ Specifically, β -keto acyl-acyl carrier protein (ACP) intermediates are diverted from fatty acid biosynthesis, hydrolyzed by methylketone synthase 2 (MKS2), followed by decarboxylation by MKS1.^{26,27} *C. elegans*, however, does not contain homologs of either protein. Conversely, in bacteria and fungi, bioengineering efforts have manipulated fatty acid β -oxidation pathways to increase the production of medium- and long-chain methyl ketones as potential biofuels. The strategies used have included deletion of a 3-ketoacyl-CoA thiolase in the β -oxidation pathway, leading to accumulation of β -keto acyl-CoA intermediates, as well as expression of the promiscuous thioesterase FadM to hydrolyze β -keto acyl-CoA intermediates for subsequent nonenzymatic decarboxylation to methyl ketones.^{28–30} Interestingly, *C. elegans daf-22* mutant strains accumulate ascarosides with long side chains that terminate in an MK moiety.³¹ However, wild-type *C. elegans* has only been shown to produce in appreciable amounts MK-containing ascarosides with 6-carbon side chains, suggesting that some other mechanism beyond downregulation of *daf-22* is needed to produce the MK-containing ascaroside pheromones. Given that β -oxidation is a central component of the ascaroside biosynthetic pathway, we hypothesized that an ACOT enzyme might play a role in the biosynthesis of MK-containing ascarosides, analogous to that of FadM (Figure 1B).

In this study, we identified an *acot* gene in *C. elegans* that is specifically involved in the biosynthesis of ascarosides that terminate in an MK moiety. Analysis of the ascarosides and ascarosyl-CoA thioesters in *acot-15* mutant and *acot-15* overexpression strains revealed that MK-containing ascarosides are produced during β -oxidation of the ascaroside side chain. Levels of the MK-containing ascarosides could be partially restored through the treatment of the *acot-15* endometabolome with base. Thus, ACOT-15 likely hydrolyzes a β -keto acyl-CoA intermediate during ascaroside β -oxidation, leading to decarboxylation and MK formation. Unbiased comparative metabolomics of wild-type and *acot-15* mutant strains enabled the discovery of other MK-containing ascarosides, as well as a structurally unique piperidyl ascaroside. While the MK-containing ascaroside asc-C6-MK (1) is a key dauer pheromone and extends lifespan, the piperidyl ascaroside is much less dauer-inducing and reduces lifespan. Although the piperidyl ascaroside is synthesized inside the worm without the aid of bacterial metabolism, the type of bacterial food provided to the worm dramatically affects the production of the piperidyl ascaroside. Our work provides a mechanism whereby food could potentially influence life history traits in the worm.

RESULTS

Ascaroside production in an *acot-15* mutant

BLAST analysis of the *C. elegans* genome suggests that it encodes four ACOT enzymes from the type I thioesterase family

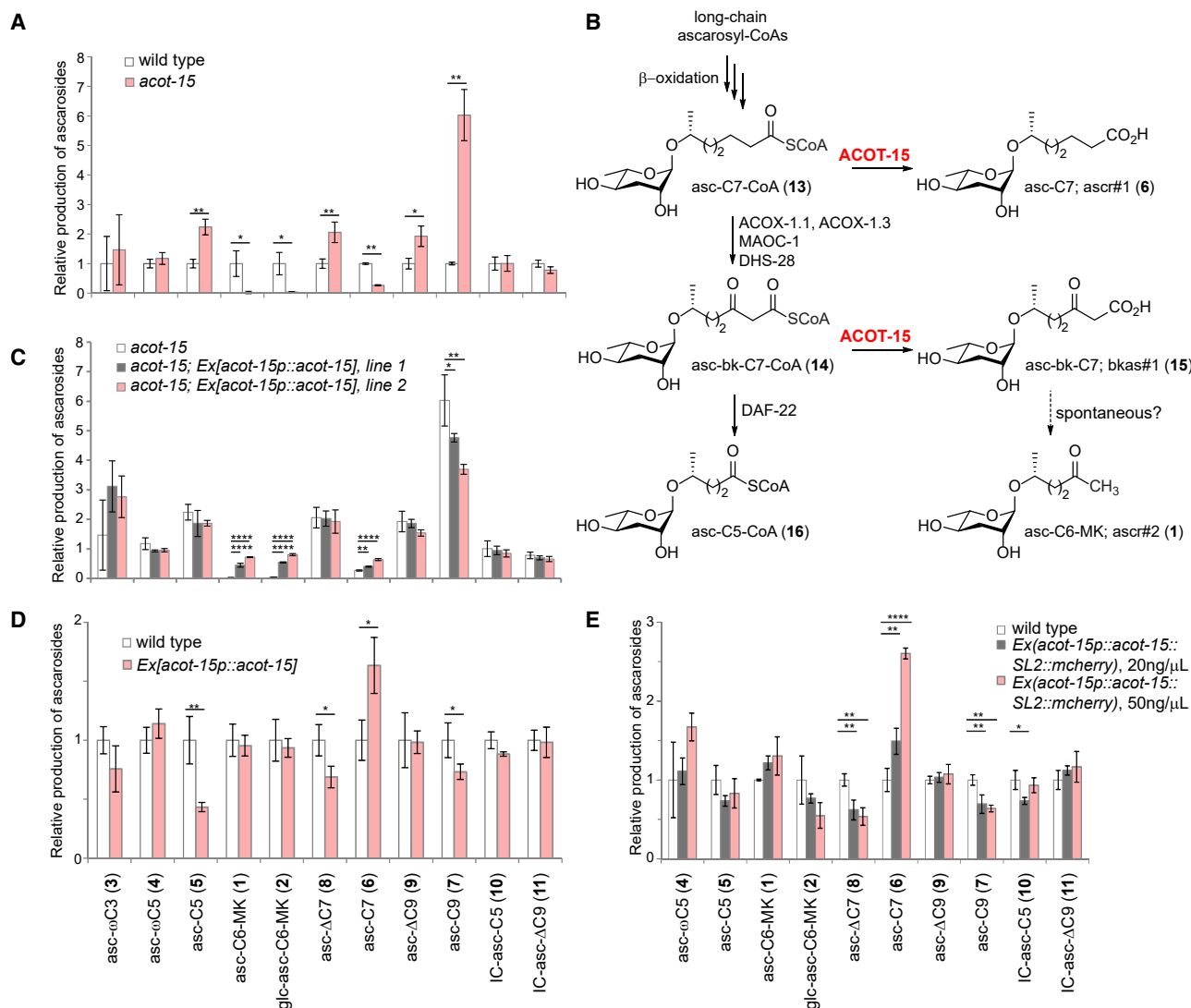


Figure 2. Ascaroside production in the *acot-15* mutant and overexpression strains

(A) The production of ascarosides by the *acot-15*(*ttT1876*) mutant relative to wild type. (B) Model for the role of ACOT-15 in the biosynthesis of asc-C6-MK (1) and asc-C7 (6). (C) The production of ascarosides in the *acot-15*(*ttT1876*) mutant upon rescue with *acot-15p::acot-15*. The ratio of the ascaroside in the mutant or rescue strain is shown relative to wild type. Two lines were generated and gave similar results. (D) The production of ascarosides in the *acot-15p::acot-15* overexpression strain relative to wild type. (E) The production of ascarosides in the *acot-15p::acot-15::SL2::mcherry* overexpression strain (generated by injecting the overexpression construct at 20 ng/μL and at 50 ng/μL) relative to wild type. In (A), (C), (D), and (E), data represent the mean ± standard deviation of three biological replicates. In (A) and (D), p values were calculated using an unpaired *t* test, and in (C) and (E), p values were calculated using one-way ANOVA with Dunnett's post hoc test (**p* ≤ 0.05, ***p* ≤ 0.01, ****p* ≤ 0.001, *****p* ≤ 0.0001).

(α/β hydrolase fold), including ACOT-1, C31H5.6, W03D8.8, and T05E7.1. We gave T05E7.1 the name ACOT-15, given that it is not directly orthologous to any of the human ACOT enzymes. Sequence alignment indicates that the *C. elegans* Type I ACOT enzymes have the catalytic triad (Asp-His-Ser), including the Gly-X-Ser-X-Gly motif, that is present in all Type I ACOT enzymes and other α/β hydrolases (Data S1). All four enzymes have variants of the peroxisomal targeting sequence (PTS-1) on their C-terminus, suggesting that they are localized to the peroxisome.³² Given that the peroxisome is an important site

for ascaroside biosynthesis, we hypothesized that they could potentially be involved in ascaroside biosynthesis. For the four Type I ACOT enzymes in *C. elegans*, a *Mos1* transposon insertion mutant strain was available for one of them, *acot-15*(*ttT1876*). Thus, we backcrossed the mutant, grew it in liquid culture, and analyzed ascaroside production by LC-MS. Surprisingly, the *acot-15*(*ttT1876*) mutant produces virtually no asc-C6-MK (1) or glc-asc-C6-MK (2), and also produces less asc-C7 (6) (Figure 2A). From these data, we hypothesized that ACOT-15 may hydrolyze the CoA group from ascarosides with β -keto-C7

side chains and, to a lesser degree, C7 side chains (Figure 2B). Once hydrolyzed, the β -keto-C7 side chains could potentially undergo decarboxylation to produce asc-C6-MK (1). Additionally, the *acot-15* mutant accumulates asc-C5 (5), asc- Δ C7 (8), asc- Δ C9 (9), and asc-C9 (7), which may reflect a redirection of metabolic flux to those ascarosides whose biosynthesis is not dependent on ACOT-15.

To confirm further that the defects in the *acot-15(ttT1876)* mutant strain were due to loss of *acot-15*, we generated a rescue strain by PCR-amplifying a segment of genomic DNA encompassing the *acot-15* promoter, coding sequence, and 3'-UTR and injecting the PCR product into the *acot-15(ttT1876)* mutant. The production of asc-C6-MK (1) and glc-asc-C6-MK (2) was completely rescued, and the production of asc-C7 (6) was partially rescued (Figure 2C). Thus, *acot-15* is required in production of these ascarosides.

Ascaroside production in an *acot-15* overexpression strain

To provide further support for the role of *acot-15* in ascaroside biosynthesis, an *acot-15* overexpression strain was generated by injecting the *acot-15* PCR product into wild-type worms. The *acot-15* overexpression strain produced asc-C7 (6) at higher levels (Figure 2D). Thus, ACOT-15 may catalyze the hydrolysis of asc-C7-CoA (13) to produce asc-C7 (6). However, overexpression of *acot-15* did not result in increased production of asc-C6-MK (1) or glc-asc-C6-MK (2). One possible explanation for this result is that the *acot-15* overexpression strain may hydrolyze most of the asc-C7-CoA (13) as soon as it is produced, such that there is less of it to be processed further through β -oxidation to generate the β -keto-C7-CoA intermediate (i.e., 14) that we postulate is necessary for the biosynthesis of asc-C6-MK (1) or glc-asc-C6-MK (2) (Figure 2B). Consistent with this hypothesis, additional ascarosides that lie downstream of asc-C7-CoA (13) in the β -oxidation pathway, such as asc-C5 (5), were produced at lower levels (Figure 2D). Another possibility is that ACOT-15 may be necessary for asc-C6-MK (1) and glc-asc-C6-MK (2) biosynthesis, but not sufficient (that is, additional enzymes, such as a decarboxylase, are required), and thus overexpression of ACOT-15 does not yield more of these compounds. If this latter hypothesis were correct, we might expect increased production of asc-bk-C7 (15) in the *acot-15* overexpression strain. However, we have been unable to detect this compound in the *acot-15* overexpression strain, likely indicating that the compound rapidly decarboxylates. As an additional means to overexpress *acot-15*, translational reporter strains were generated by injecting the *acot-15p::acot-15::SL2::mcherry* reporter at either 20 or 50 ng/ μ L (Figure 2E). These data show a similar pattern to that seen in Figure 2D; that is, increasing amounts of asc-C7 (6), but similar amounts of asc-C6-MK (1) and glc-asc-C6-MK (2), were produced with increasing amounts of injected reporter.

Unbiased comparative metabolomics of wild-type and *acot-15* endometabolomes

To determine how the *acot-15* loss-of-function affects intermediates in the ascaroside β -oxidation pathway, we analyzed the endometabolome (internal metabolites) of wild-type and *acot-15* worms by LC-high resolution (HR)-MS/MS. To enable the analysis of the CoA-thioesters of various ascarosides, which are diffi-

cult to detect, we treated the samples with hydroxylamine using a protocol similar to that developed by Yu et al.²² Specific hydroxylamine derivatives were identified based on their high resolution mass, fragmentation pattern, relative retention time, absence in samples that were not treated with hydroxylamine, and the synthesis of select standards (Figures 3A and 3B, Data S2). We found that the intermediates that we predicted to be hydrolyzed by ACOT-15, asc-C7-CoA (13) and asc-bk-C7-CoA (14), are strongly downregulated in the *acot-15* endometabolome, whereas other ascarosyl-CoAs are largely not affected (see Figures 2B, 3A, and 3B). This result, which runs counter to our initial expectation, could indicate that metabolic flux in the *acot-15* mutant strain is directed away from electrophilic intermediates that might otherwise accumulate. Surprisingly, we detected a significant amount of asc-C6-MK-OX (25) in the *acot-15* endometabolome treated with hydroxylamine, and we verified the identity of this compound utilizing a standard (Figure 3C). However, the presence of asc-C6-MK-OX (25) is not due to hydroxylamine-labeling of asc-C6-MK (1), since the latter compound is not present in the control sample that was not treated with hydroxylamine (Figures 3C and 3D). We hypothesize that hydroxylamine treatment facilitates non-enzymatically the reaction that is normally catalyzed enzymatically by ACOT-15 (that is, hydrolysis of the CoA-thioester asc-bk-C7-CoA (14)). To test this hypothesis, we showed that treatment of the *acot-15* endometabolome with basic conditions can rescue some production of asc-C6-MK (1) (Figure 3E). Hydroxylamine-treated *acot-15* samples did not contain any derivatives of asc-C6-MK-OX (25), such as glucosylated derivatives (26) or phosphorylated derivatives (27), which suggests that the biosynthesis of glucosylated and phosphorylated derivatives of asc-C6-MK (1) (that is, the biosynthesis of 2 and 28) in *C. elegans* occurs through direct glycosylation/phosphorylation of asc-C6-MK, rather than modification of a biosynthetic precursor to asc-C6-MK (Figures 3F and 3G).

Unbiased comparative metabolomics of the wild-type and *acot-15* exometabolomes

To screen more broadly for secondary metabolites that are dependent on *acot-15*, we grew synchronized wild-type and *acot-15* mutant worms to the adult stage, analyzed the exometabolome (secreted metabolites) of these worms by LC-HR-MS/MS in both negative and positive mode and performed unbiased, comparative metabolomics using the commercial software MetaboScape. This software was used for all data processing steps, including retention time alignment, feature detection, and statistical analysis. Features with multiple isotopes and/or adducts were combined either automatically by the software or manually. Differential features were identified by generating volcano plots for the ESI^{+/−} data, in which the log fold-change for each feature in wild-type versus *acot-15* is plotted on the x axis and the statistical significance is plotted on the y axis (Figure 4). Initially, we focused on those metabolites that are present in wild-type and completely absent from the *acot-15* mutant strain, as we hypothesized that these metabolites are more likely to be directly biosynthesized by ACOT-15. These metabolites include asc-C6-MK (1) and glc-asc-C6-MK (2), as well as a phosphorylated derivative of asc-C6-MK (28) (Figure 4, Data S3). 2'-phosphorylated derivatives of other ascarosides have been identified previously in *C. elegans*, but their function is unknown.³³

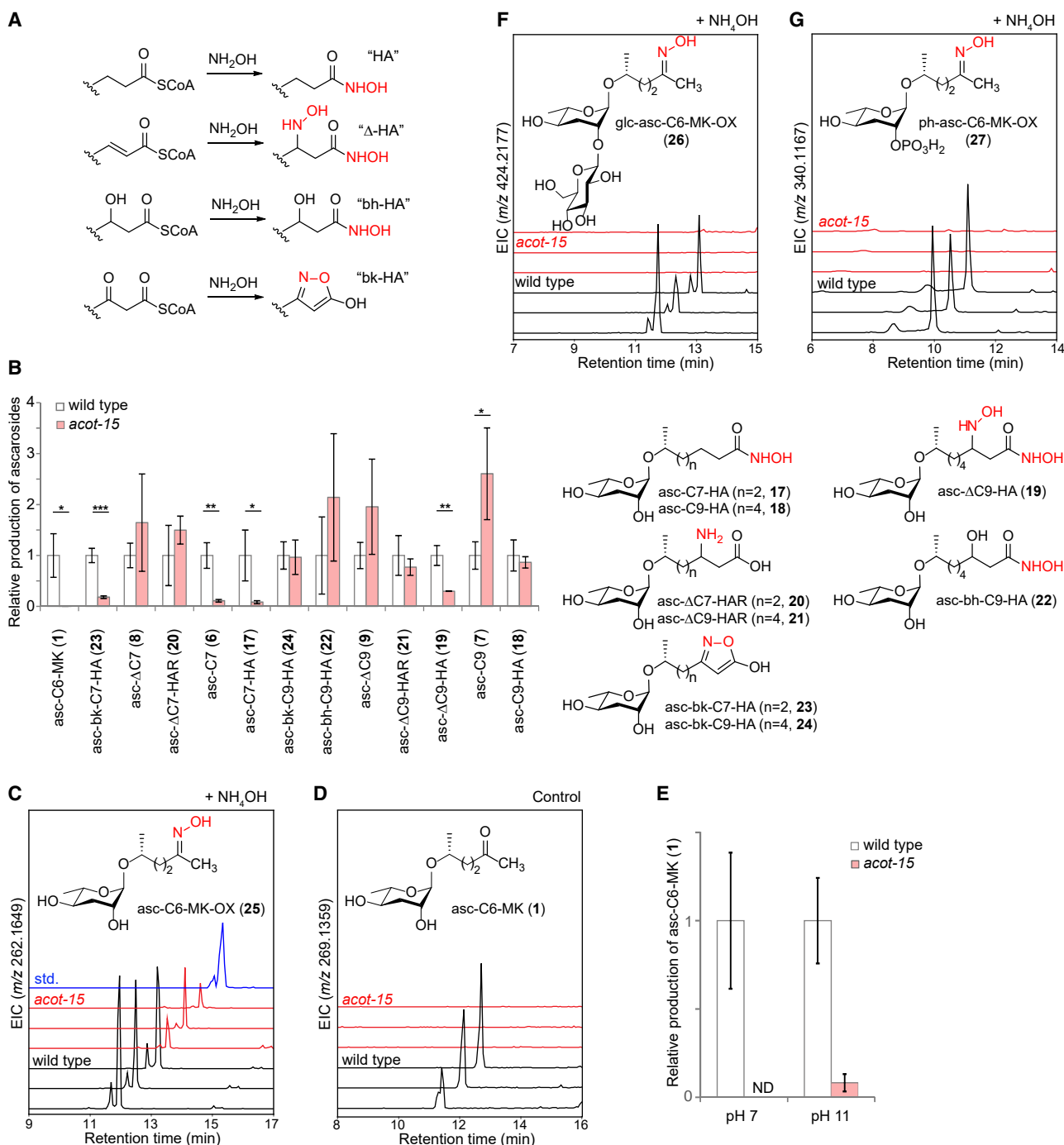


Figure 3. Analysis of the hydroxylamine-treated endometabolome of wild-type versus *acot-15* mutant worms

(A) Examples of different CoA-thioesters reacted with hydroxylamine (HA), including HA-modified saturated side chains (HA), HA-modified α,β -unsaturated side chains (Δ -HA), HA-modified β -hydroxy side chains (bh-HA), and HA-modified β -keto side chains (bk-HA).

(B) The production of ascarosides and HA-modified ascarosides in the endometabolome of *acot-15* mutant worms relative to wild-type worms, with relevant structures shown below. HA-modified α,β -unsaturated side chains where the HA group has been reduced are referred to as " Δ -HAR" (e.g., 20, 21). Data represent the mean \pm standard deviation of three biological replicates, and p values were calculated using an unpaired *t* test ($^*p \leq 0.05$, $^{**}p \leq 0.01$, $^{***}p \leq 0.001$).

(C) Extracted ion chromatogram of asc-C6-MK-OX (25) in the HA-treated wild-type and *acot-15* endometabolomes.

(D) Extracted ion chromatogram of asc-C6-MK (1) in the wild-type and *acot-15* endometabolomes.

(E) Relative amounts of asc-C6-MK (1) in the wild-type and *acot-15* endometabolomes prepared under neutral or basic conditions. Data represent the mean \pm standard deviation of three biological replicates.

(F) Extracted ion chromatogram of glc-asc-C6-MK-OX (26) in the HA-treated wild-type and *acot-15* endometabolomes.

(G) Extracted ion chromatogram of ph-asc-C6-MK-OX (27) in the HA-treated wild-type and *acot-15* endometabolomes. For (B), (C), (F), and (G), see Data S2.

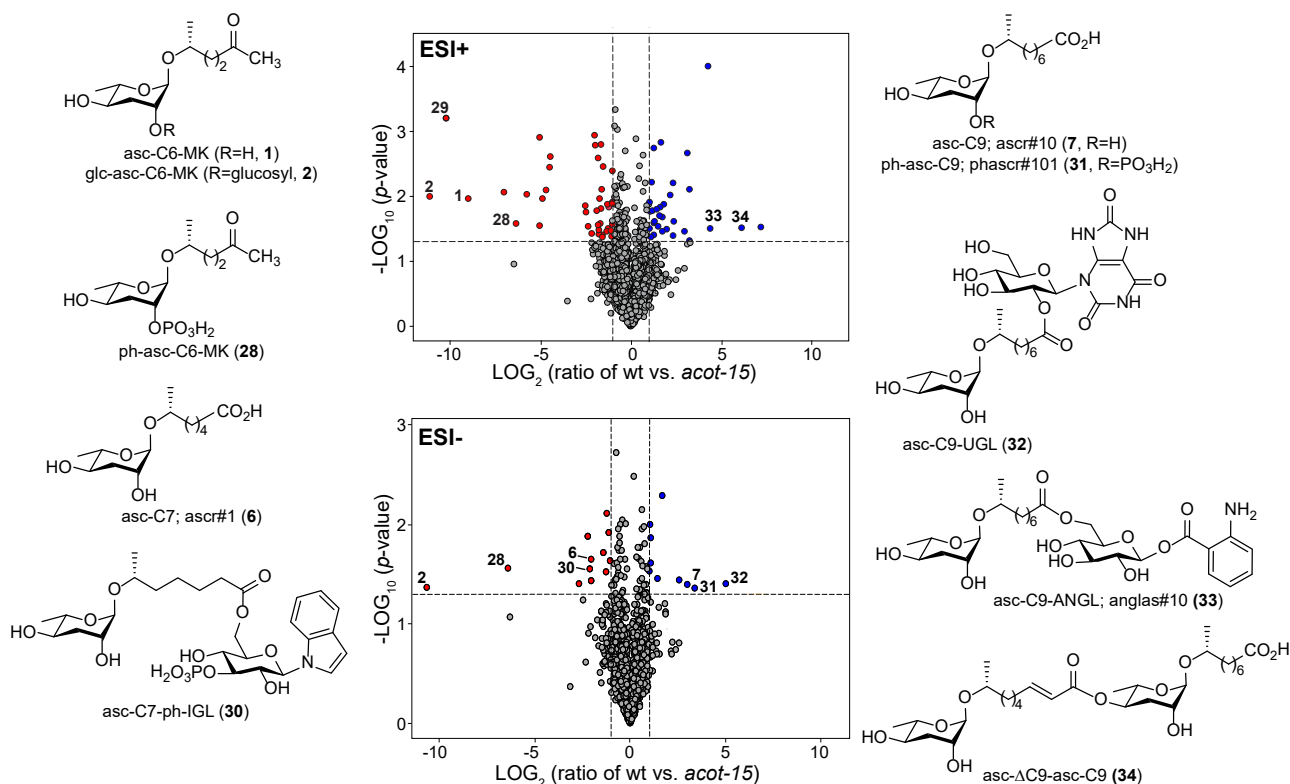


Figure 4. Comparative metabolomics of the exometabolome of wild-type versus *acot-15* mutant worms

Volcano plots of wild-type versus *acot-15* (*ttT1876*) exometabolome analyzed in positive (ESI+) (top) and negative mode (ESI-) (bottom). Fold change is indicated on the x axis, with mass features that are less abundant in the *acot-15* exometabolome toward the left and those that are more abundant toward the right. Statistical significance (p value) is indicated on the y axis. Highlighted features in the volcano plot are numbered, and these numbers correspond to the numbers indicated for the ascaroside structures. The chemical structures are proposed based on the fragmentation pattern by LC-HR-MS/MS. Some features could not be further characterized due to low signal and/or absence of fragmentation by LC-HR-MS/MS. See [Data S3](#). The chemical structure of **29** is elucidated in [Figure 5](#).

Furthermore, we identified an additional ascaroside that was completely absent in the *acot-15* mutant strain (**29** in [Figure 4](#)) with a structure that could not be easily deduced from MS data (see next section for structure elucidation).

Our earlier experiments suggested that the *acot-15* loss-of-function mutant reduces flux through the β -oxidation pathway of ascarosides with 9-carbon side chains to those with shorter side chains. The *acot-15* exometabolome was depleted in asc-C7 (**6**), as well as a derivative of asc-C7 with a phosphorylated indole glucoside group (**30**), suggesting that flux to asc-C7-CoA (**13**) is reduced and/or that ACOT-15 contributes to the hydrolysis of asc-C7-CoA (**13**) ([Figure 4](#), [Data S3](#)). Conversely, the *acot-15* exometabolome showed the accumulation of ascarosides with 9-carbon side chains. These include asc-C9 (**7**), as well as asc-C9 derivatives modified with a phosphoryl group (**31**), uric acid gluconucleoside group (**32**), the anthralic acid glucosyl group (**33**), or another ascaroside (**34**) ([Figure 4](#), [Data S3](#)).

Structural characterization of a piperidyl ascaroside

We detected a structurally unique ascaroside in the wild-type exometabolome (**29** in [Figure 4](#)), which is completely absent in the *acot-15* exometabolome and has a molecular formula of $C_{17}H_{31}NO_5$. The MS² spectrum of the ascaroside suggested that

it contains a piperidine group ($C_5H_{11}N$) and that this group is likely attached to the side chain of the ascaroside ([Figure 5A](#)). Despite our extensive efforts to optimize a high-performance liquid chromatography (HPLC) method to purify the compound, the compound did not produce a sharp peak. Thus, we adopted a purification strategy that did not rely on HPLC and that utilized C18, followed by silica gel, then sephadex LH-20 chromatography. Based on the isolated amount of the compound, it is present in the mid-nanomolar range in the culture medium, which is roughly similar to the concentration of asc-C6-MK (**1**). NMR characterization indicated that the chemical shifts of this ascaroside are highly similar to those of asc-C6-MK (**1**), except for those at the very end of the side chain. NMR characterization also confirmed the presence of a piperidine group and its attachment to the terminus of the side chain ([Figure 5B](#); [Table S1](#), [Data S4](#)). Thus, we named this ascaroside modified with a piperidine (pip) group, asc-C6-pip (**29**). The NMR data of the side-chain terminus of asc-C6-pip (**29**) are very similar to the NMR data of the alkaloids pelletierine (**35**) and anaferine (**36**).³⁴ Like asc-C6-pip (**29**), these alkaloids also display a strong piperidine fragment in their MS² spectra.³⁵ The complex splitting pattern of the protons at positions C-1, C-3, and C-1'' suggests that we isolated a mixture of two epimers at C-1'' ([Figure 5C](#); [Table S1](#), [Data S4](#)). Indeed, the stereocenter in pelletierine has been reported to undergo racemization through a

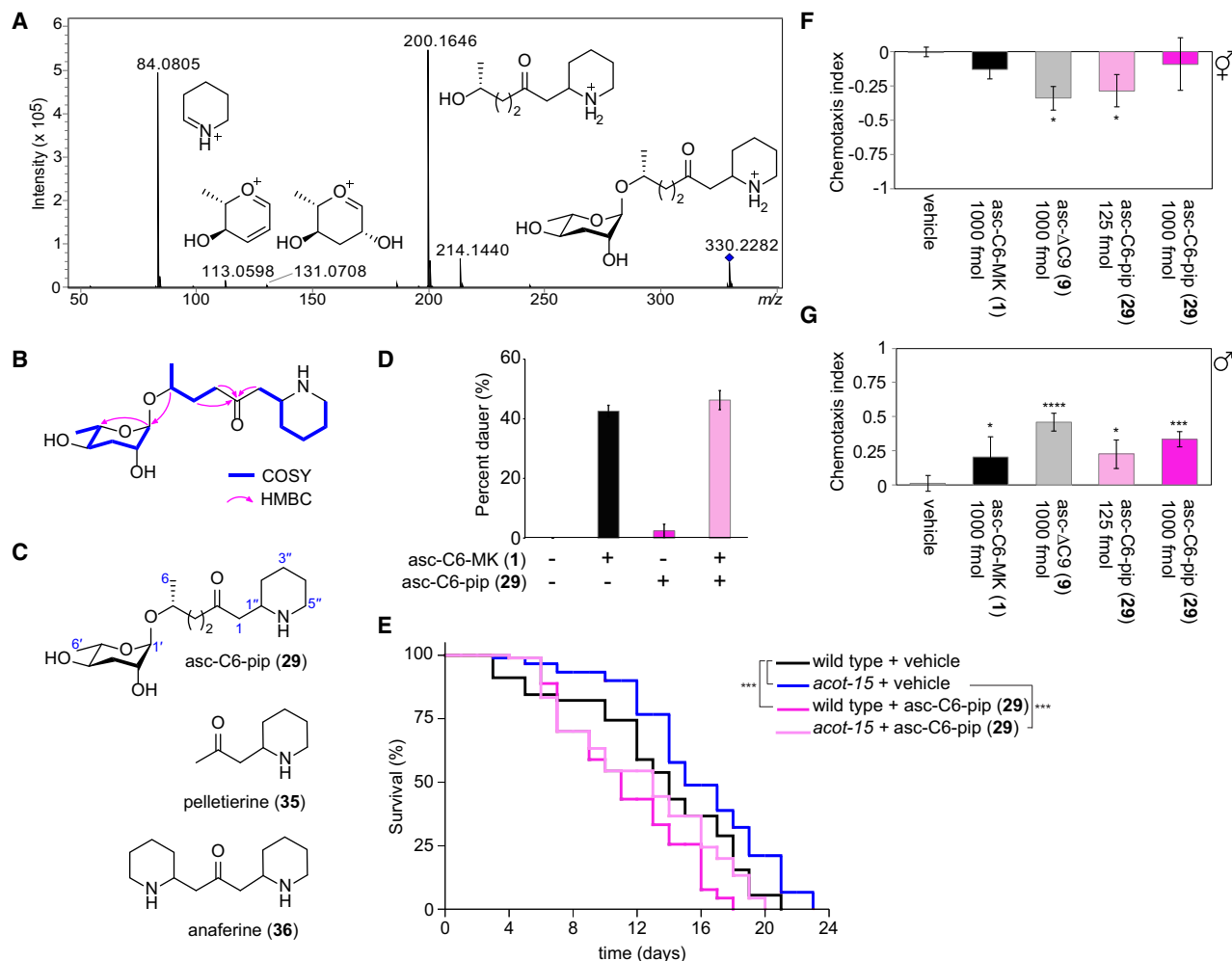


Figure 5. Structural characterization of an ascarioside with a piperidine ring

(A) MS/MS fragmentation pattern of asc-C6-pip (29) analyzed in positive mode (ESI+).
 (B) Key NMR correlations from COSY and HMBC spectra of asc-C6-pip (29). See [Data S4](#) and [Table S1](#).
 (C) The structure of asc-C6-pip (29), with the structures of the alkaloids pelletierine (35) and anaferine (36) for comparison.
 (D) Dauer formation assay in response to asc-C6-MK (1) and asc-C6-pip (29).
 (E) Lifespan assay in response to asc-C6-pip (29) in both wild-type and *acot-15* (*ttT1876*) worms.
 (F and G) Chemotaxis assay with different ascariosides in hermaphrodites (F) and males (G). In (D), (F), and (G), data represent the mean \pm standard deviation of three biological replicates. In (F) and (G), p values were calculated using one-way ANOVA with Dunnett's post hoc test, and in (E), p values were calculated using a log rank test (* $p \leq 0.05$, ** $p \leq 0.01$, *** $p \leq 0.001$, **** $p \leq 0.0001$).

retro aza-Michael reaction.³⁶ Thus, it is possible that asc-C6-pip (29) is either biosynthesized as a diastomeric mixture or that it is biosynthesized as an enantiomerically pure compound that undergoes racemization at C-1'' during purification.

Interestingly, unlike asc-C6-MK (1), asc-C6-pip (29), does not have strong dauer-inducing activity (Figure 5D). Thus, regulation of the biosynthesis of the piperidine group might serve as a means to control dauer activity in the worm. In contrast to asc-C6-MK (1), which was previously reported to extend lifespan in wild-type worms, asc-C6-pip (29) shortens lifespan in both wild-type worms and *acot-15* mutant worms (Figure 5E).³⁷ The *acot-15* mutant worms themselves, which do not produce either asc-C6-MK (1) or asc-C6-pip (29), live slightly longer than wild-type worms (Figure 5E). In chemotaxis assays, asc-C6-pip (29) is slightly repellent to hermaphrodites, but only at

lower concentrations, and is attractive to males (Figures 5F and 5G).

Biosynthetic model for the piperidyl ascarioside

We have proposed a biosynthetic pathway for asc-C6-pip (29) that is based on the biosynthetic pathway of pelletierine (35) (Figure 6). Pelletierine is a well-known alkaloid from *Punica granatum* (pomegranate) and is also a key building block for the Lycopodium alkaloids, a large family of psychoactive alkaloids produced by club mosses.^{38,39} The biosynthesis of pelletierine begins with the production by a polyketide synthase of 3-oxoglutaryl-CoA.³⁵ Although the mechanism is not well understood, the polyketide synthase is thought to catalyze a decarboxylative condensation between the 3-oxoglutaryl group bound to the enzyme and 1-piperidine (Figure 6A). Hydrolysis of the thioester

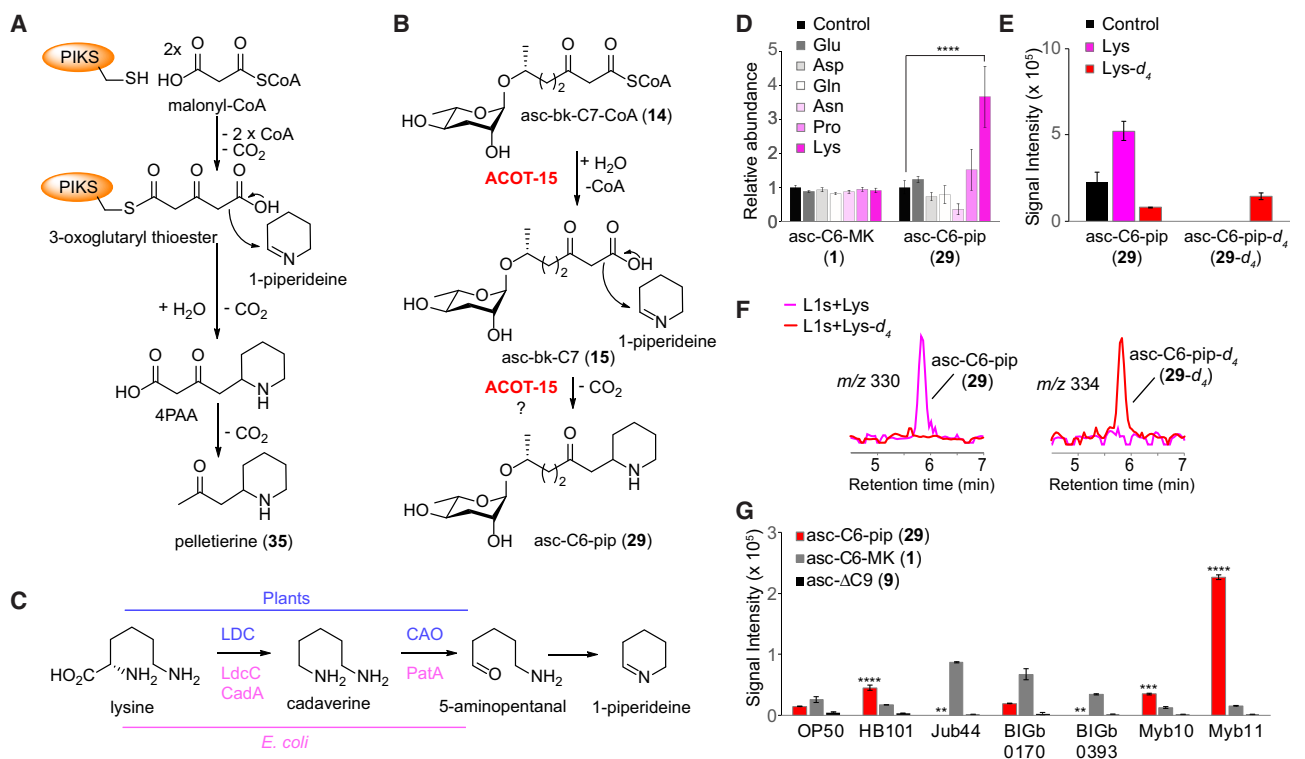


Figure 6. Biosynthesis of pelletierine and asc-C6-pip

(A) Biosynthetic pathway to pelletierine (35).

(B) Proposed biosynthetic pathway to asc-C6-pip (29).

(C) Biosynthetic pathway to 1-piperideine in club mosses (top) and bacteria (bottom).

(D) Relative ascaroside production in mixed stage wild-type worms fed bacteria supplemented with different amino acids.

(E) Unlabeled and labeled asc-C6-pip (29) production in wild-type worms fed bacterial powder supplemented with unlabeled and labeled lysine.

(F) Extracted ion chromatograms for unlabeled and labeled asc-C6-pip (29) produced by arrested L1 worms treated with unlabeled and labeled lysine in the absence of bacterial food.

(G) Production of asc-C6-pip (29) and other ascarosides in wild-type worms fed either OP50, HB101, or various bacterial strains isolated from the *C. elegans* microbiome. Data represent the mean \pm standard deviation of two biological replicates (E and G) or three biological replicates (D). In (D) and (G), p values were calculated using one-way ANOVA with Dunnett's post hoc test (* $p \leq 0.05$, ** $p \leq 0.01$, *** $p \leq 0.001$, **** $p \leq 0.0001$). In (G), p values are only shown for asc-C6-pip (29) for the different bacterial strains relative to the control bacteria (OP50).

to generate 4-(2-piperidyl)acetoacetic acid (4PAA), followed by decarboxylation, then generates pelletierine (35). In a similar fashion, our model proposes that a β -keto ascaroside, asc-bk-C7 (15), generated by ACOT-15 undergoes a decarboxylative condensation with 1-piperideine to generate asc-C6-pip (29), through either an enzymatic or nonenzymatic process (Figure 6B).

The biosynthesis of 1-piperideine has not been studied in the worm, but has been studied in plants and bacteria. In club mosses, lysine decarboxylase (LDC) converts lysine to cadaverine, which is converted by copper amine oxidase (CAO) to 5-aminopentanal that spontaneously cyclizes to form 1-piperideine (Figure 6C). In *E. coli*, the lysine decarboxylases LdcC and CadA convert lysine to cadaverine, and the putrescine transaminase PatA serves as a cadaverine transaminase (Figure 6C).^{40,41} The 1-piperideine in the asc-C6-pip (29) biosynthetic pathway is likely derived from lysine, since feeding *C. elegans* cultures with lysine, but not other amino acids, led to increased production of asc-C6-pip (29) (Figure 6D). To determine whether *C. elegans* biosynthesizes 1-piperideine itself or obtains

1-piperideine from its *E. coli* diet, we fed *C. elegans* *E. coli* powder, which had been processed through sonication and lyophilization, plus either unlabeled or labeled lysine. *C. elegans* was able to incorporate the labeling into asc-C6-pip (29), indicating that asc-C6-pip biosynthesis utilizes lysine, occurs within the worm, and does not require bacterial metabolism (Figure 6E). Growth of *C. elegans* on *E. coli* mutants defective in 1-piperideine biosynthesis did not affect production asc-C6-pip (29), confirming that asc-C6-pip biosynthesis does not utilize 1-piperideine made by bacteria (Figure S1A). In further support of the hypothesis that *C. elegans* synthesizes 1-piperideine *de novo* for biosynthesis of asc-C6-pip (29), we were able to observe this ascaroside in the exometabolome of arrested first stage (L1) larvae (Figure S1B). These arrested L1 larvae were obtained by hatching washed *C. elegans* eggs in the absence of bacterial food, and thus, any metabolites observed in the L1 exometabolome are likely made by the worm. When labeled lysine was added to arrested L1 larvae in the absence of bacterial food, the worms were able to biosynthesize labeled asc-C6-pip (29) (Figure 6F), further confirming that the metabolite is made within the worm, without help from

bacteria. Attempts to identify the genes in *C. elegans* that are required for 1-piperideine production, however, were unsuccessful (Figure S1C).

Despite the fact that asc-C6-pip (**29**) is made within the worm without help from bacteria, the bacterial food provided to the worm influences the amount of the pheromone produced by the worm. To characterize this phenomenon, we fed wild-type worms a panel of different bacterial foods, including the standard laboratory strains OP50 and HB101, as well as several bacterial strains previously isolated from the *C. elegans* microbiome.⁴² Arrested L1 larvae, which were generated from wild-type hermaphrodites grown on OP50, were cultured with the different bacterial strains until the worms reached the adult stage, and ascaroside production was then analyzed (Figure 6G). Interestingly, the amount of asc-C6-pip (**29**) that the worms produced varied dramatically depending on which bacterial strain the worms were fed. This result suggests that bacterial food may indirectly affect the biosynthetic pathway in *C. elegans* that produces asc-C6-pip (**29**).

DISCUSSION

Here, we have identified an acyl-CoA thioesterase, ACOT-15, that is required for the biosynthesis of a key component of the *C. elegans* dauer pheromone, asc-C6-MK (**1**), as well as several other MK-containing ascarosides and a piperidyl-modified ascaroside, asc-C6-pip (**29**). This discovery represents the first example of a naturally occurring biosynthetic pathway to methyl ketones that involves β -oxidation. Plants synthesize MK natural products utilizing a pathway that is based on fatty acid biosynthesis, not β -oxidation; specifically, in tomato, MKS2 hydrolyzes a β -keto fatty acyl-ACP, followed by decarboxylation by MKS1.^{26,27} Previous use of β -oxidation pathways to produce MK-containing pathways were engineered, not naturally occurring pathways.^{28–30}

Multiple lines of evidence suggest that MK-containing ascarosides in *C. elegans* are produced by termination of β -oxidation through hydrolysis of a β -keto ascarosyl-CoA (specifically asc-bk-C7-CoA, **14**) by ACOT-15. In our earlier work, we showed that asc-C6-MK (**1**) biosynthesis likely occurs during the round of β -oxidation that shortens a 7-carbon ascarosyl-CoA (asc-C7-CoA, **13**) to a 5-carbon ascarosyl-CoA (asc-C5-CoA, **16**). This round of β -oxidation specifically utilizes the acyl-CoA oxidases ACOX-1.1 and ACOX-1.3 (see Figure 2B) to install α,β -unsaturation.^{18,19} Relative to wild type, *acox-1.1* and *acox-1.3* mutant worms show increased production of asc-C7 (**6**) relative to asc- Δ C7 (**8**), as well as reduced production other downstream ascarosides, including asc-C6-MK (**1**). Furthermore, conditions that downregulated the expression of *acox-1.3*, specifically addition of bacterial food, resulted in reduced production of downstream ascarosides, including asc-C6-MK (**1**).¹⁸

Our comparative metabolomics data indicate that *acot-15* is required for the biosynthesis of asc-C6-MK (**1**) and contributes to the production of asc-C7 (**6**). Specifically, deletion of *acot-15* eliminates production of asc-C6-MK (**1**), glc-asc-C6-MK (**2**), additional MK-containing ascarosides, and asc-C6-pip (**29**), and reduces production of asc-C7 (**6**). On the other hand, overexpression only leads to increased production of asc-C7 (**6**), not asc-C6-MK (**1**). This result is likely due to any asc-C7-CoA (**13**) produced being hydrolyzed to asc-C7 and thus diverted away

from further β -oxidation and subsequent production of asc-C6-MK (**1**) and other downstream ascarosides. As established through hydroxylamine treatment of the endometabolome of the *acot-15* mutant, there is reduced production of the precursors to asc-C6-MK (**1**) and asc-C7 (**6**) (that is, asc-bk-C7-CoA, **14**, and asc-C7-CoA, **13**, respectively), possibly through some feedback mechanism. This shift in flux through the β -oxidation pathway contributes to the additional changes in ascaroside production seen in the mutant. Indeed, the *acot-15* exometabolome shows moderate decreases in various asc-C7 (**6**) derivatives and moderate increases in various asc-C9 (**7**) derivatives. ACOT-15 likely functions by hydrolyzing the thioester of asc-bk-C7-CoA (**14**), as well as possibly by hydrolyzing the thioester of asc-C7-CoA (**13**). Despite extensive efforts, we have been unable to express ACOT-15 in *E. coli* to enable purification and enzymatic assay. Thus, we are so far unable to directly confirm the activity of ACOT-15. However, the rescue of the production of asc-C6-MK (**1**) in the *acot-15* endometabolome through treatment with base supports our model for ACOT-15 in the hydrolysis of asc-bk-C7-CoA (**14**).

Regulation of ACOT-15 expression likely plays an important role in controlling the production of dauer pheromone in *C. elegans*. Expression profiling experiments have shown that *acot-15* is highly expressed in well-fed larval stage worms, especially the L2 and L3 stages, and downregulated in predaughters and dauers, possibly indicating that the worm reduces dauer pheromone production once it has committed to dauer.⁴³ Consistent with these data, *acot-15* has been shown to be strongly downregulated in TGF- β mutants as they enter dauer, relative to wild-type worms that were not undergoing the dauer transition.⁴⁴ Also consistent with these data, *acot-15* has been shown to be downregulated in *daf-9* mutants after commitment to dauer.⁴⁵ Our previous data show that the production of asc-C6-MK (**1**) correlates with the expression levels of *acot-15*. This pheromone is produced in similar amounts in early larval stage worms regardless of whether they are grown under dauer-inducing or non-dauer-inducing conditions.¹⁸ However, once the dauer-inducing conditions lead to the formation of pre-dauers, production of asc-C6-MK (**1**), as well as many other ascarosides, is suppressed in dauer-inducing conditions while it continues to rise in non-dauer-inducing conditions.¹⁸ However, *acot-15* is upregulated in *daf-7* mutant adults, suggesting that regulation of *acot-15* may be different in adults.⁴⁶ Interestingly, exposure of hermaphrodites to males has been shown to upregulate *acot-15* in the hermaphrodites, but the functional consequences of this upregulation are unclear.⁴⁷

Intriguingly, we have discovered an ascaroside derivative containing a piperidine ring (asc-C6-pip, **29**) that is biosynthesized via an ACOT-15-dependent mechanism. In plants, biosynthesis of pelletierine requires a polyketide synthase that is proposed to react an enzyme-bound 3-oxoglutaryl moiety with 1-piperideine to produce 4PAA, which then undergoes decarboxylation (Figure 6A).³⁵ In the biosynthesis of asc-C6-pip (**29**), we propose a model in which ACOT-15 utilizes its active-site serine to hydrolyze the thioester of asc-bk-C7-CoA (**14**) to generate a β -keto acid. This β -keto acid then reacts with 1-piperideine through either an enzymatic or nonenzymatic process, although we favor the former since the nonenzymatic reaction of acetoacetic acid with 1-piperideine proceeds slowly at neutral pH.³⁵ Alternatively,

it is conceivable that asc-bk-C7-CoA (**14**) reacts with 1-piperidine, and then ACOT-15 catalyzes the hydrolysis of the CoA-thioester, enabling decarboxylation and generating asc-C6-pip (**29**). Interestingly, we did not detect any asc-C6-pip (**29**) in the endometabolome. This result may suggest that asc-C6-pip (**29**) is produced in small amounts, that it is rapidly exported outside the worm, or that its biosynthesis is completed outside the worm.

While asc-C6-MK (**1**) is a key component of the dauer pheromone, asc-C6-pip (**29**) does not promote dauer formation. Thus, the piperidyl derivative may be produced under conditions where it would be less beneficial to enter dauer. The two pheromones also contrast in terms of their effects on lifespan with asc-C6-MK (**1**) extending lifespan and asc-C6-pip (**29**) reducing it.³⁷ Interestingly, we have established that asc-C6-pip (**29**) is biosynthesized by the worm without the help of bacterial metabolism and that the worm uses lysine to build the piperidine ring of asc-C6-pip (**29**). Despite the ability of the worm to make asc-C6-pip (**29**) on its own, the type of bacterial food that the worm consumes appears to impact the production of this pheromone by the worm. While the mechanism is unclear, bacterial food may affect the availability of lysine for biosynthesis of asc-C6-pip (**29**) or may affect indirectly the enzymatic machinery inside the worm that constructs the pheromone. Thus, we may have uncovered a potential mechanism whereby food impacts chemical signaling in the worm.

Limitations of the study

Since we have been unable to heterologously express and purify ACOT-15 for enzymatic assays, we have not been able to directly study its role in the biosynthesis of asc-C6-MK (**1**) and asc-C6-pip (**29**). Additionally, we hypothesize that asc-C6-pip (**29**) may be biosynthesized through the reaction of a β -keto acid generated by ACOT-15 with piperidine, but we have yet to confirm this mechanism beyond showing that asc-C6-pip biosynthesis utilizes lysine. Future studies will need to further explore the biological role of asc-C6-pip (**29**), as well as how the bacterial food source influences the biosynthesis of this ascaroside inside the worm.

SIGNIFICANCE

Nematodes communicate with a family of pheromones known as the ascarosides that help the worm to coordinate diverse aspects of its development and behavior. During pheromone biosynthesis, the side chains of the ascarosides are shortened through β -oxidation, but the mechanism by which this process is terminated is poorly understood. MK-containing ascarosides represent essential components of several pheromones in *C. elegans*. Here, we identify an acyl-CoA thioesterase, ACOT-15, that is required for the biosynthesis of MK-containing ascarosides, including the important dauer pheromone asc-C6-MK (1**). We propose a model in which ACOT-15 hydrolyzes the β -keto acyl-CoA side chain of an ascaroside intermediate during β -oxidation, leading to decarboxylation and formation of the MK moiety. The biosynthesis of MK-containing metabolites has only been characterized in one other system, plants, where intermediates in fatty acid biosynthesis, specifically β -keto fatty**

acyl groups linked to acyl carrier proteins, are diverted to make the MK metabolites. Thus, ACOT-15 represents the first enzyme that generates an MK in the context of a β -oxidation pathway. Using unbiased comparative metabolomics of wild type versus the *acot-15* mutant, we identify additional ACOT-15-dependent pheromones, including a piperidyl-modified ascaroside, asc-C6-pip (29**), which is reminiscent of pelletierine, a key building block to the *Lycopodium* alkaloids. The β -keto acid generated by ACOT-15 likely couples to 1-piperidine to produce the piperidyl ascaroside. Unlike asc-C6-MK (**1**), which promotes dauer and extends lifespan, asc-C6-pip (**29**) is not significantly dauer-inducing and shortens lifespan. We demonstrate that worms biosynthesize the piperidine ring in asc-C6-pip (**29**) from lysine, without the help of bacterial metabolism. Surprisingly, however, the type of bacterial food provided to the worm dramatically affects the production in the worm of asc-C6-pip (**29**) and may thereby affect chemical signaling in the worm.**

STAR★METHODS

Detailed methods are provided in the online version of this paper and include the following:

- KEY RESOURCES TABLE
- RESOURCE AVAILABILITY
 - Lead contact
 - Materials availability
 - Data and code availability
- EXPERIMENTAL MODEL AND STUDY PARTICIPANT DETAILS
 - *C. elegans* strains
 - Bacterial strains
- METHOD DETAILS
 - *acot-15* rescue strain
 - *acot-15* overexpression strains
 - Unsynchronized worm cultures
 - LC-MS analysis
 - Extraction of the endometabolome and hydroxylamine labeling
 - Synthesis of ascarosides
 - Synthesis of standards for hydroxylamine-labeled compounds
 - Synchronized worm cultures for comparative metabolomics of the exometabolome
 - LC-HR-MS/MS analysis
 - Processing of comparative metabolomics data
 - Purification and structure elucidation of asc-C6-pip (**29**)
 - Dauer formation
 - Lifespan assay
 - Chemotaxis assay
 - Ascaroside analysis for worm cultures supplemented with different amino acids
 - Preparation of bacterial powder
 - Ascaroside analysis for worm cultures supplemented with labeled lysine
 - Ascaroside analysis for worms grown on bacterial mutant strains

- Ascaroside analysis for worms grown on *C. elegans* microbiome strains

- QUANTIFICATION AND STATISTICAL ANALYSIS

SUPPLEMENTAL INFORMATION

Supplemental information can be found online at <https://doi.org/10.1016/j.chembiol.2023.12.006>.

ACKNOWLEDGMENTS

We would like to thank Jim Rocca for his help with obtaining NMR spectra. A portion of this work was performed in the McKnight Brain Institute at the National High Magnetic Field Laboratory's Advanced Magnetic Resonance Imaging and Spectroscopy (AMRIS) Facility, which is supported by National Science Foundation Cooperative Agreement DMR-2128556 and the State of Florida. We acknowledge Laurent Segalat (Centre National de la Recherche Scientifique, Lyon, France) and members of the NemaGENETAG consortium for generating and providing the *Mos1* strain. Some bacterial strains were provided by the National BioResource Project (Japan). LC-HR-MS/MS analysis was performed at the University of Florida Mass Spectrometry Research and Education Center, which is funded by the National Institutes of Health (S10 OD021758-01A1). This work was supported by the National Science Foundation (CHE-1555050) and the National Institutes of Health (R35 GM114076).

AUTHOR CONTRIBUTIONS

S.B., C.-S.Y., and R.A.B. conceived the study and analyzed data; J.H., S.B., and C.L.S. generated worm strains; S.B., J.H., Y.W., and C.-S.Y. performed targeted metabolomics; S.B. and D.V.P. performed comparative metabolomics; S.B., D.V.P., L.S.B. and K.B.B. analyzed comparative metabolomics data; C.-S.Y. purified and characterized the structure of novel metabolites; K.M. performed biological assays; R.A.B. wrote the manuscript, which was edited and approved by all authors.

DECLARATION OF INTERESTS

The authors declare no competing interests.

Received: April 3, 2023

Revised: September 2, 2023

Accepted: December 10, 2023

Published: January 5, 2024

REFERENCES

1. Butcher, R.A., Fujita, M., Schroeder, F.C., and Clardy, J. (2007). Small-molecule pheromones that control dauer development in *Caenorhabditis elegans*. *Nat. Chem. Biol.* 3, 420–422.
2. Butcher, R.A., Ragains, J.R., Kim, E., and Clardy, J. (2008). A potent dauer pheromone component in *C. elegans* that acts synergistically with other components. *Proc. Natl. Acad. Sci. USA* 105, 14288–14292.
3. Butcher, R.A., Ragains, J.R., and Clardy, J. (2009). An indole-containing dauer pheromone component with unusual dauer inhibitory activity at higher concentrations. *Org. Lett.* 11, 3100–3103.
4. Srinivasan, J., Kaplan, F., Ajredini, R., Zachariah, C., Alborn, H.T., Teal, P.E.A., Malik, R.U., Edison, A.S., Sternberg, P.W., and Schroeder, F.C. (2008). A blend of small molecules regulates both mating and development in *Caenorhabditis elegans*. *Nature* 454, 1115–1118.
5. Pungalaya, C., Srinivasan, J., Fox, B.W., Malik, R.U., Ludewig, A.H., Sternberg, P.W., and Schroeder, F.C. (2009). A shortcut to identifying small molecule signals that regulate behavior and development in *Caenorhabditis elegans*. *Proc. Natl. Acad. Sci. USA* 106, 7708–7713.
6. Srinivasan, J., von Reuss, S.H., Bose, N., Zaslaver, A., Mahanti, P., Ho, M.C., O'Doherty, O.G., Edison, A.S., Sternberg, P.W., and Schroeder, F.C. (2012). A modular library of small molecule signals regulates social behaviors in *Caenorhabditis elegans*. *PLoS Biol.* 10, e1001237.
7. Izrayelit, Y., Srinivasan, J., Campbell, S.L., Jo, Y., von Reuss, S.H., Genoff, M.C., Sternberg, P.W., and Schroeder, F.C. (2012). Targeted metabolomics reveals a male pheromone and sex-specific ascaroside biosynthesis in *Caenorhabditis elegans*. *ACS Chem. Biol.* 7, 1321–1325.
8. Artyukhin, A.B., Yim, J.J., Srinivasan, J., Izrayelit, Y., Bose, N., von Reuss, S.H., Jo, Y., Jordan, J.M., Baugh, L.R., Cheong, M., et al. (2013). Succinylated octopamine ascarosides and a new pathway of biogenic amine metabolism in *Caenorhabditis elegans*. *J. Biol. Chem.* 288, 18778–18783.
9. Greene, J.S., Brown, M., Dobosiewicz, M., Ishida, I.G., Macosko, E.Z., Zhang, X., Butcher, R.A., Cline, D.J., McGrath, P.T., and Bargmann, C.I. (2016). Balancing selection shapes density-dependent foraging behaviour. *Nature* 539, 254–258.
10. Zhang, X., Noguez, J.H., Zhou, Y., and Butcher, R.A. (2013). Analysis of ascarosides from *Caenorhabditis elegans* using mass spectrometry and NMR spectroscopy. *Methods Mol. Biol.* 1068, 71–92.
11. Jeong, P.Y., Jung, M., Yim, Y.H., Kim, H., Park, M., Hong, E., Lee, W., Kim, Y.H., Kim, K., and Paik, Y.K. (2005). Chemical structure and biological activity of the *Caenorhabditis elegans* dauer-inducing pheromone. *Nature* 433, 541–545.
12. Dong, C., Reilly, D.K., Bergame, C., Dolke, F., Srinivasan, J., and von Reuss, S.H. (2018). Comparative ascaroside profiling of *Caenorhabditis* exometabolomes reveals species-specific (ω) and (ω -2)-hydroxylation downstream of peroxisomal β -oxidation. *J. Org. Chem.* 83, 7109–7120.
13. Cohen, S.M., Wrobel, C.J.J., Prakash, S.J., Schroeder, F.C., and Sternberg, P.W. (2022). Formation and function of dauer ascarosides in the nematodes *Caenorhabditis briggsae* and *Caenorhabditis elegans*. *G3* 12.
14. Butcher, R.A., Ragains, J.R., Li, W., Ruvkun, G., Clardy, J., and Mak, H.Y. (2009). Biosynthesis of the *Caenorhabditis elegans* dauer pheromone. *Proc. Natl. Acad. Sci. USA* 106, 1875–1879.
15. Joo, H.J., Yim, Y.H., Jeong, P.Y., Jin, Y.X., Lee, J.E., Kim, H., Jeong, S.K., Chitwood, D.J., and Paik, Y.K. (2009). *Caenorhabditis elegans* utilizes dauer pheromone biosynthesis to dispose of toxic peroxisomal fatty acids for cellular homeostasis. *Biochem. J.* 422, 61–71.
16. Joo, H.J., Kim, K.Y., Yim, Y.H., Jin, Y.X., Kim, H., Kim, M.Y., and Paik, Y.K. (2010). Contribution of the peroxisomal *acox* gene to the dynamic balance of daumone production in *Caenorhabditis elegans*. *J. Biol. Chem.* 285, 29319–29325.
17. von Reuss, S.H., Bose, N., Srinivasan, J., Yim, J.J., Judkins, J.C., Sternberg, P.W., and Schroeder, F.C. (2012). Comparative metabolomics reveals biogenesis of ascarosides, a modular library of small-molecule signals in *C. elegans*. *J. Am. Chem. Soc.* 134, 1817–1824.
18. Zhang, X., Feng, L., Chinta, S., Singh, P., Wang, Y., Nunnery, J.K., and Butcher, R.A. (2015). Acyl-CoA oxidase complexes control the chemical message produced by *Caenorhabditis elegans*. *Proc. Natl. Acad. Sci. USA* 112, 3955–3960.
19. Zhang, X., Wang, Y., Perez, D.H., Jones Lipinski, R.A., and Butcher, R.A. (2018). Acyl-CoA oxidases fine-tune the production of ascaroside pheromones with specific side chain lengths. *ACS Chem. Biol.* 13, 1048–1056.
20. Zhou, Y., Xia, X.M., Lingle, C.J., Bhar, S., Jones Lipinski, R.A., Han, J., Feng, L., and Butcher, R.A. (2018). Biosynthetic tailoring of existing ascaroside pheromones alters their biological function in *C. elegans*. *Elife* 7, e38060.
21. Hunt, M.C., Siponen, M.I., and Alexson, S.E.H. (2012). The emerging role of acyl-CoA thioesterases and acyltransferases in regulating peroxisomal lipid metabolism. *Biochim. Biophys. Acta* 1822, 1397–1410.
22. Yu, Y., Le, H.H., Curtis, B.J., Wrobel, C.J.J., Zhang, B., Maxwell, D.N., Pan, J.Y., and Schroeder, F.C. (2020). An untargeted approach for revealing electrophilic metabolites. *ACS Chem. Biol.* 15, 3030–3037.
23. Williams, W.G., Kennedy, G.G., Yamamoto, R.T., Thacker, J.D., and Bordner, J. (1980). 2-Tridecanone: A naturally occurring insecticide from

- the wild tomato *Lycopersicon hirsutum* f. *glabratum*. *Science* 207, 888–889.
24. Mason, R.T., Fales, H.M., Jones, T.H., Pannell, L.K., Chinn, J.W., and Crews, D. (1989). Sex pheromones in snakes. *Science* 245, 290–293.
 25. Fridman, E., Wang, J., Iijima, Y., Froehlich, J.E., Gang, D.R., Ohlrogge, J., and Pichersky, E. (2005). Metabolic, genomic, and biochemical analyses of glandular trichomes from the wild tomato species *Lycopersicon hirsutum* identify a key enzyme in the biosynthesis of methylketones. *Plant Cell* 17, 1252–1267.
 26. Auldridge, M.E., Guo, Y., Austin, M.B., Ramsey, J., Fridman, E., Pichersky, E., and Noel, J.P. (2012). Emergent decarboxylase activity and attenuation of alpha/beta-hydrolase activity during the evolution of methylketone biosynthesis in tomato. *Plant Cell* 24, 1596–1607.
 27. Yu, G., Nguyen, T.T.H., Guo, Y., Schauvinhold, I., Auldridge, M.E., Bhuiyan, N., Ben-Israel, I., Iijima, Y., Fridman, E., Noel, J.P., and Pichersky, E. (2010). Enzymatic functions of wild tomato methylketone synthases 1 and 2. *Plant Physiol.* 154, 67–77.
 28. Goh, E.B., Baidoo, E.E.K., Keasling, J.D., and Beller, H.R. (2012). Engineering of bacterial methyl ketone synthesis for biofuels. *Appl. Environ. Microbiol.* 78, 70–80.
 29. Goh, E.B., Baidoo, E.E.K., Burd, H., Lee, T.S., Keasling, J.D., and Beller, H.R. (2014). Substantial improvements in methyl ketone production in *E. coli* and insights on the pathway from in vitro studies. *Metab. Eng.* 26, 67–76.
 30. Hanks, E.K.R., Denby, C.M., Sánchez I Nogué, V., Lin, W., Ramirez, K.J., Singer, C.A., Beckham, G.T., and Keasling, J.D. (2018). Engineering β -oxidation in *Yarrowia lipolytica* for methyl ketone production. *Metab. Eng.* 48, 52–62.
 31. Izrayelit, Y., Robinette, S.L., Bose, N., von Reuss, S.H., and Schroeder, F.C. (2013). 2D NMR-based metabolomics uncovers interactions between conserved biochemical pathways in the model organism *Caenorhabditis elegans*. *ACS Chem. Biol.* 8, 314–319.
 32. Hunt, M.C., Nousiainen, S.E., Huttunen, M.K., Orii, K.E., Svensson, L.T., and Alexson, S.E. (1999). Peroxisome proliferator-induced long chain acyl-CoA thioesterases comprise a highly conserved novel multi-gene family involved in lipid metabolism. *J. Biol. Chem.* 274, 34317–34326.
 33. Hoki, J.S., Le, H.H., Mellott, K.E., Zhang, Y.K., Fox, B.W., Rodrigues, P.R., Yu, Y., Helf, M.J., Baccile, J.A., and Schroeder, F.C. (2020). Deep interrogation of metabolism using a pathway-targeted click-chemistry approach. *J. Am. Chem. Soc.* 142, 18449–18459.
 34. Bonandi, E., Tedesco, G., Perdicchia, D., and Passarella, D. (2020). Total synthesis of (-)-anaferine: A further ramification in a diversity-oriented approach. *Molecules* 25, 1057.
 35. Nett, R.S., Dho, Y., Low, Y.Y., and Sattely, E.S. (2021). A metabolic regulon reveals early and late acting enzymes in neuroactive Lycopodium alkaloid biosynthesis. *Proc. Natl. Acad. Sci. USA* 118, e2102949118.
 36. Monaco, M.R., Renzi, P., Scarpino Schietroma, D.M., and Bella, M. (2011). Biomimetic organocatalytic asymmetric synthesis of 2-substituted piperidine-type alkaloids and their analogues. *Org. Lett.* 13, 4546–4549.
 37. Ludewig, A.H., Izrayelit, Y., Park, D., Malik, R.U., Zimmermann, A., Mahanti, P., Fox, B.W., Bethke, A., Doering, F., Riddle, D.L., and Schroeder, F.C. (2013). Pheromone sensing regulates *Caenorhabditis elegans* lifespan and stress resistance via the deacetylase SIR-2.1. *Proc. Natl. Acad. Sci. USA* 110, 5522–5527.
 38. Wibaut, J.P., and Hollstein, U. (1957). Investigation of the alkaloids of *Punica granatum* L. *Arch. Biochem. Biophys.* 69, 27–32.
 39. Ma, X., and Gang, D.R. (2004). The Lycopodium alkaloids. *Nat. Prod. Rep.* 21, 752–772.
 40. Knorr, S., Sinn, M., Galetskiy, D., Williams, R.M., Wang, C., Müller, N., Mayans, O., Schleheck, D., and Hartig, J.S. (2018). Widespread bacterial lysine degradation proceeding via glutarate and L-2-hydroxyglutarate. *Nat. Commun.* 9, 5071.
 41. Samsonova, N.N., Smirnov, S.V., Altman, I.B., and Ptitsyn, L.R. (2003). Molecular cloning and characterization of *Escherichia coli* K12 *ygjG* gene. *BMC Microbiol.* 3, 2.
 42. Dirksen, P., Assié, A., Zimmermann, J., Zhang, F., Tietje, A.M., Marsh, S.A., Félix, M.A., Shapira, M., Kaleta, C., Schulenburg, H., and Samuel, B.S. (2020). CeMbio - The *Caenorhabditis elegans* Microbiome Resource. *G3 (Bethesda)* 10, 3025–3039.
 43. Gerstein, M.B., Lu, Z.J., Van Nostrand, E.L., Cheng, C., Arshinoff, B.I., Liu, T., Yip, K.Y., Robilotto, R., Rechtsteiner, A., Ikegami, K., et al. (2010). Integrative analysis of the *Caenorhabditis elegans* genome by the modENCODE project. *Science* 330, 1775–1787.
 44. Liu, T., Zimmerman, K.K., and Patterson, G.I. (2004). Regulation of signaling genes by TGF β during entry into dauer diapause in *C. elegans*. *BMC Dev. Biol.* 4, 11.
 45. Lee, J.S., Shih, P.Y., Schaedel, O.N., Quintero-Cadena, P., Rogers, A.K., and Sternberg, P.W. (2017). FMRamide-like peptides expand the behavioral repertoire of a densely connected nervous system. *Proc. Natl. Acad. Sci. USA* 114, E10726–E10735.
 46. Shaw, W.M., Luo, S., Landis, J., Ashraf, J., and Murphy, C.T. (2007). The *C. elegans* TGF β dauer pathway regulates longevity via insulin signaling. *Curr. Biol.* 17, 1635–1645.
 47. Booth, L.N., Shi, C., Tantilert, C., Yeo, R.W., Miklas, J.W., Hebestreit, K., Hollenhorst, C.N., Maures, T.J., Buckley, M.T., Murphy, C.T., and Brunet, A. (2022). Males induce premature demise of the opposite sex by multifaceted strategies. *Nat. Aging* 2, 809–823.
 48. Miyabayashi, T., Palfreyman, M.T., Sluder, A.E., Slack, F., and Sengupta, P. (1999). Expression and function of members of a divergent nuclear receptor family in *Caenorhabditis elegans*. *Dev. Biol.* 215, 314–331.
 49. Mello, C.C., Kramer, J.M., Stinchcomb, D., and Ambros, V. (1991). Efficient gene transfer in *C. elegans*: extrachromosomal maintenance and integration of transforming sequences. *EMBO J.* 10, 3959–3970.
 50. Iliff, A.J., Wang, C., Ronan, E.A., Hake, A.E., Guo, Y., Li, X., Zhang, X., Zheng, M., Liu, J., Grosh, K., et al. (2021). The nematode *C. elegans* senses airborne sound. *Neuron* 109, 3633–3646.e7.
 51. Hollister, K.A., Conner, E.S., Zhang, X., Spell, M., Bernard, G.M., Patel, P., de Carvalho, A.C.G.V., Butcher, R.A., and Ragains, J.R. (2013). Ascaroside activity in *Caenorhabditis elegans* is highly dependent on chemical structure. *Bioorg. Med. Chem.* 21, 5754–5769.
 52. Faghieh, N., Bhar, S., Zhou, Y., Dar, A.R., Mai, K., Bailey, L.S., Basso, K.B., and Butcher, R.A. (2020). A large family of enzymes responsible for the modular architecture of nematode pheromones. *J. Am. Chem. Soc.* 142, 13645–13650.
 53. Shi, C., Runnels, A.M., and Murphy, C.T. (2017). Mating and male pheromone kill *Caenorhabditis* males through distinct mechanisms. *Elife* 6, e23493.

STAR★METHODS

KEY RESOURCES TABLE

REAGENT or RESOURCE	SOURCE	IDENTIFIER
Bacterial and virus strains		
<i>E. coli</i> : OP50	Caenorhabditis Genetics Center (CGC)	RRID: WB-STRAIN: WBStrain00041969
<i>E. coli</i> : HB101	Caenorhabditis Genetics Center (CGC)	RRID: WB-STRAIN: WBStrain00041075
<i>E. coli</i> : BW25113	National BioResource Project	N/A
<i>E. coli</i> : JW0181 Δ ldcC::kan	National BioResource Project	N/A
<i>E. coli</i> : JW4092 Δ cadA::kan	National BioResource Project	N/A
<i>E. coli</i> : JW5510 Δ patA::kan	National BioResource Project	N/A
<i>Sphingobacterium</i> sp.: BIGb0170	Caenorhabditis Genetics Center (CGC)	RRID: WB-STRAIN: WBStrain00047213
<i>Chryseobacterium</i> sp.: Jub44	Caenorhabditis Genetics Center (CGC)	RRID: WB-STRAIN: WBStrain00047335
<i>Acinetobacter guillouiae</i> : MYb10	Caenorhabditis Genetics Center (CGC)	RRID: WB-STRAIN: WBStrain00047356
<i>Pseudomonas lurida</i> : MYb11	Caenorhabditis Genetics Center (CGC)	RRID: WB-STRAIN: WBStrain00047357
<i>Pantoea</i> sp.: BIGb0393	Caenorhabditis Genetics Center (CGC)	RRID: WB-STRAIN: WBStrain00047215
Chemicals, peptides, and recombinant proteins		
lysine- <i>d</i> ₄ ·HCl	C/D/N Isotopes	Cat# D-2554
Deposited data		
Metabolomics data	This paper	MassIVE: MSV000092618 MassIVE: MSV000092620
Experimental models: Organisms/strains		
<i>C. elegans</i> : N2, Bristol	Caenorhabditis Genetics Center (CGC)	RRID: WB-STRAIN: WBStrain00000001
<i>C. elegans</i> : RAB90 <i>acot-15</i> (ttT1876)	NemaGENETAG Consortium, then backcrossed 6 times in this paper	N/A
<i>C. elegans</i> : RAB115 <i>acot-15</i> (ttT1876); <i>rebEx29</i> (<i>acot-15p</i> :: <i>acot-15</i> , 50ng/uL; <i>coel</i> :: <i>dsRed</i>)	This paper	N/A
<i>C. elegans</i> : RAB119 <i>rebEx29</i> (<i>acot-15p</i> :: <i>acot-15</i> , 50ng/uL; <i>coel</i> :: <i>dsRed</i>)	This paper	N/A
<i>C. elegans</i> : RAB117 <i>rebEx31</i> (<i>acot-15p</i> :: <i>acot-15</i> :: <i>sl2</i> :: <i>mcherry</i> , 20ng/uL; <i>rol-6</i> (<i>su1006</i>))	This paper	N/A
<i>C. elegans</i> : RAB118 <i>rebEx32</i> (<i>acot-15p</i> :: <i>acot-15</i> :: <i>sl2</i> :: <i>mcherry</i> , 50ng/uL; <i>rol-6</i> (<i>su1006</i>))	This paper	N/A
<i>C. elegans</i> : VC40475, million mutation strain, contains many mutations including <i>odc-1</i> (<i>gk655931</i>)	Caenorhabditis Genetics Center (CGC)	RRID: WB-STRAIN: WBStrain00039456
<i>C. elegans</i> : F53F10.2(<i>tm5730</i>)	National BioResource Project	N/A
<i>C. elegans</i> : <i>oatr-1</i> (<i>tm4545</i>)	National BioResource Project	N/A
Oligonucleotides		
Primer for amplifying <i>acot-15</i> from genomic DNA: <i>acot-15_PCR_for</i> : TGGGTTAGTACAA TATAATCTATATAACAGG	This paper	N/A
Primer for amplifying <i>acot-15</i> from genomic DNA: <i>acot-15_PCR_rev</i> : TCATCTCTTCTTG ATCTTCGCGATT	This paper	N/A

(Continued on next page)

Continued

REAGENT or RESOURCE	SOURCE	IDENTIFIER
Primer for amplifying <i>acot-15</i> from genomic DNA and inserting into pBS77-SL2-mCherry2: <i>acot-15_reporter_for</i> : CGCGGATCCGGGTTA GTACAATATAATCTAT	This paper	N/A
Primer for amplifying <i>acot-15</i> from genomic DNA and inserting into pBS77-SL2-mCherry2: <i>acot-15_reporter_rev</i> : CATGGCTAGCCCGCC GCTCCATTTTCTTTGTTT	This paper	N/A
Recombinant DNA		
<i>coel::RFP</i>	Miyabayashi et al. ⁴⁸	Addgene plasmid #8938
<i>pRF4::rol-6(su1006)</i>	Mello et al. ⁴⁹	RRID: WB-ID: WBCnstr00004720
pBS77-SL2-mCherry2	Iliff et al. ⁵⁰	N/A
pBS77- <i>acot-15p::acot15-SL2-mCherry2</i>	This paper	N/A
Software and algorithms		
Metaboscope, version 5.0	Bruker	N/A
GraphPad Prism, version 9.0	GraphPad Software	N/A
Other		
Sephadex LH-20	Sigma	Cat# LH20100
Sep-Pak tC18 3 cc Vac Cartridge, 200 mg Sorbent per Cartridge, 37-55 μ m	Waters	Cat# 186004618
Luna 5 μ m C18 2 100 \AA (100 x 4.6 mm) column	Phenomenex	Cat# 00D-4252E0
Hypersil GOLD aQ Polar Endcapped C18 3 μ m 175 \AA (2.1 x 150 mm) column	ThermoFisher	Cat# 25303-152130

RESOURCE AVAILABILITY**Lead contact**

Further information and requests for materials are directed to the lead contact, Rebecca A. Butcher (butcher@chem.ufl.edu).

Materials availability

There are restrictions to the availability of *asc-C6-pip* (**29**) due to the low quantity of the material remaining after completion of this work. However, a detailed procedure for isolating *asc-C6-pip* (**29**) is included in the “[purification and structure elucidation of *asc-C6-pip* \(**29**\)](#)” section in the [STAR Methods](#). All other unique materials newly generated in this study are available upon request from the [lead contact](#).

Data and code availability

- The mass spectrometry datasets generated during this study have been deposited at MassIVE mass spectrometry data repository and are publicly available. The accession numbers are listed in the [key resources table](#).
- This paper does not report original code.
- Any additional information required to reanalyze the data reported in this paper is available from the [lead contact](#) upon request.

EXPERIMENTAL MODEL AND STUDY PARTICIPANT DETAILS***C. elegans* strains**

Strains used in this study include wild type (N2, Bristol), RAB90 *acot-15(ttT876)*, RAB115 *acot-15(ttT876)*; *rebEx29(acot-15p::acot-15, 50ng/uL; coel::dsRed)*, RAB119 *rebEx29(acot-15p::acot-15, 50ng/uL; coel::dsRed)*; RAB117 *rebEx31(acot-15p::acot-15::SL2::mcherry, 20ng/uL; rol-6(su1006))*, and RAB118 *rebEx32(acot-15p::acot-15::SL2::mcherry, 50ng/uL; rol-6(su1006))*. The RAB90 strain was backcrossed six times, and the VC40475 *odc-1(gk655931)*, F53F10.2(*tm5730*), and *oatr-1(tm4545)* strains were used without backcrossing.

Bacterial strains

The BW25113 (wild-type), JW0181 (*ldcC*), JW4092 (*cadA*), and JW5510 (*patA*) bacterial strains were obtained from the National BioResource Project of Japan. The BIGb0170, Jub44, MYb10, MYb11, and BIGb0393 bacterial strains were obtained from the *Caenorhabditis* Genetics Center.

METHOD DETAILS

acot-15 rescue strain

To generate the *acot-15* rescue strain RAB115, 5.3 kb of genomic DNA, including the *acot-15* gene and 2 kb upstream and 323 bp downstream, was amplified by PCR using primers *acot-15_PCR_for* and *acot-15_PCR_rev*. The PCR product (at 50 ng/μL), along with *coel::dsRed* marker DNA (at 50 ng/μL), was injected into the RAB90 *acot-15(ttTi876)* strain to generate RAB115 *acot-15(ttTi876); rebEx29(acot-15p::acot-15; coel::dsRed)*. Two independent lines of the rescue strain were generated.

acot-15 overexpression strains

To generate the *acot-15* overexpression strain RAB119, 5.3 kb of genomic DNA, including the *acot-15* gene and 2 kb upstream and 323 bp downstream, was amplified by PCR using primers *acot-15_PCR_for* and *acot-15_PCR_rev*. The PCR product (at 50 ng/μL), along with *coel::dsRed* marker DNA (at 50 ng/μL), was injected into wild-type worms to generate RAB119 *rebEx29(acot-15p::acot-15, 50ng/μL; coel::dsRed)*. To generate the RAB117 and RAB118 strains, the genomic region containing promoter, gene sequence and 3'-UTR for *acot-15* (5.1 kb) was amplified from *C. elegans* genomic DNA using primers *acot-15_reporter_for* and *acot-15_reporter_rev* and inserted into pBS77-SL2-mCherry plasmid⁵⁰ at the *Bam*HI/*Nhe*I sites. The resulting translational reporter plasmid was injected into wild-type worms at different concentrations (20 or 50 ng/μL). The pRF4::*rol-6(su1006)* plasmid⁴⁹ (20 ng/μL) was used as an co-injection marker and an empty plasmid (pUC18) was used to adjust the total DNA concentration of the injection mix to 100 ng/μL.

Unsynchronized worm cultures

For Figure 2A, large-scale (150 mL) nonsynchronized worm cultures were fed *E. coli* (OP50) and grown for 9 d, and extracts were generated from the culture medium, as described.¹⁰ For small scale (5 mL) nonsynchronized worm cultures in Figures 2C–2E, worms were grown on a NGM agar plate (6 cm) at 20°C until the bacterial food on the plate was almost gone. Then, the plate was washed with 5 mL of S medium and transferred to 50 mL culture tube (day 1). The worms were grown at 22.5°C for 6 d and were fed with 500 μL of 25X OP50 every 2 d (days 1, 3, and 5) in Figures 2C and 2D or every day in Figure 2E. For sample collection in these experiments, the culture was incubated in an ice-bath for 30 min to 1 h to settle the worms, and the supernatant was centrifuged (2,675 g for 10 min). 1 mL of this supernatant was lyophilized and resuspended in 100 μL of 50% (v/v) methanol in water, and the ascarosides were analyzed by LC-MS.

LC-MS analysis

LC-MS analysis of ascarosides was performed on a Phenomenex Luna 5 μm C₁₈ (2) 100 Å (100 x 4.6 mm) column attached to an Agilent 1260 infinity binary pump and Agilent 6130 single quad mass spectrometer with API-ES source, operating in dual negative/positive single-ion monitoring mode. A water (with 0.1% formic acid) and acetonitrile (with 0.1% formic acid) solvent gradient was used, holding at 5% acetonitrile for 5 min, ramping to 60% acetonitrile over 20 min, ramping to 100% acetonitrile, and then holding at 100% acetonitrile for 4 min. In general, all ascarosides were detected by LC-MS using the [M-H]⁻ ion, except for asc-C6-MK (1) and glc-asc-C6-MK (2), which were detected using their [M+Na]⁺ ion.

Extraction of the endometabolome and hydroxylamine labeling

Hydroxylamine labelling experiments were performed similar to the method of Yu et al.²² with the following changes. 200,000 synchronized starved L1 worms were inoculated into 25 mL S medium in a 250 mL Erlenmeyer flask supplemented with 2% (w/v) 25X HB101. The worms were grown in a shaker at 22.5°C at 220 rpm, and 5 mL of 25X HB101 (100 mg/mL) was added every 24 h. After 60 h, the cultures were each transferred to 50 mL tubes and centrifuged. Each worm pellet was washed once with 40 mL of autoclaved water and then washed twice with 40 mL of 0.1 X PBS solution (pH 7). After discarding the supernatant, the recovered 5 mL of wet volume of worm pellet from each tube was divided equally between two 15 mL tubes, for control and hydroxylamine treatment. 10 mL of 0.1 X PBS (pH 7) was added to the control set, and 10 mL of 100 mM NH₂OH in 0.1X PBS (pH 7) was added to the treatment set. Immediately upon the addition (within 10 s) the solution was mixed with the worm pellet by inverting two times followed by worm lysis. A microfluidizer was used to lyse the worms at 18,000 psi for 5 cycles. Following worm lysis, the samples were frozen at -80°C overnight and then lyophilized to dryness. The dried samples were extracted with 15 mL of methanol, evaporated using a rotary evaporator, and resuspended in 500 μL of methanol for analysis by LC-HR-MS/MS.

Synthesis of ascarosides

(*R*)-5-(((2*R*,3*R*,5*R*,6*S*)-3,5-dihydroxy-6-methyltetrahydro-2*H*-pyran-2-yl)oxy)octan-2-one, asc-C6-MK (1), and (*R*,*E*)-8-(((2*R*,3*R*,5*R*,6*S*)-3,5-dihydroxy-6-methyltetrahydro-2*H*-pyran-2-yl)oxy)non-2-enoic acid, asc-ΔC9 (9), were synthesized exactly as described by Hollister et al., utilizing dibenzoyl ascaryleose synthesized using the method of Jeong et al.^{11,51} ¹H NMR for asc-C6-MK (1) (400 MHz, MeOD) δ 4.63 (s, 1H), 3.79 (ddd, *J* = 8.0, 6.3, 4.7 Hz, 1H), 3.70 (td, *J* = 3.1, 1.5 Hz, 1H), 3.59–3.47 (m, 2H), 2.62 (t, *J* = 7.4 Hz, 2H), 2.15 (s, 3H), 1.95 (dt, *J* = 13.1, 3.3 Hz, 1H), 1.81–1.66 (m, 3H), 1.21 (d, *J* = 5.6 Hz, 3H), 1.13 (d, *J* = 6.1 Hz, 3H). ¹H NMR for asc-ΔC9 (9) (400 MHz, MeOD) δ 6.93 (dt, *J* = 14.1, 6.9 Hz, 1H), 5.80 (d, *J* = 15.7 Hz, 1H), 4.63 (s, 1H), 3.78 (m, 1H), 3.70 (s, 1H), 3.61 (dq, *J* = 9.4, 6.3 Hz, 1H), 3.50 (ddd, *J* = 11.2, 9.4, 4.5 Hz, 1H), 2.23 (q, *J* = 6.6 Hz, 2H), 1.94 (dt, *J* = 12.9, 4.0 Hz, 1H), 1.75 (m, 1H), 1.60–1.38 (m, 6H), 1.20 (d, *J* = 6.3 Hz, 3H), 1.11 (d, *J* = 6.1 Hz, 3H). These ¹H-NMR data matched those of the previously synthesized compounds.

Synthesis of standards for hydroxylamine-labeled compounds

10 μ L of asc-C6-MK (**1**, 10 μ g dissolved in ethanol) or asc- Δ C9 (**9**, 10 μ g dissolved in ethanol) was added to 1 mL of 0.1 M $\text{NH}_2\text{OH} \cdot \text{HCl}$ in 0.1X PBS (pH = 7). The reactions were shaken at 200 rpm at 22 °C for 48 h. The mixtures were evaporated and lyophilized, and then extracted with 1 mL of methanol. The extracts were clarified via centrifugation and analyzed by LC-HR-MS/MS. The retention times of asc-C6-MK-OX (**25**) and asc- Δ C9-HAR (**21**) matched those of the corresponding peaks in the $\text{NH}_2\text{OH} \cdot \text{HCl}$ -treated natural samples. asc-C6-MK-OX (**25**), HR-ESIMS (m/z): $[\text{M}+\text{H}]^+$ calcd. for $\text{C}_{12}\text{H}_{24}\text{NO}_5$ 262.1649; found 262.1655; asc- Δ C9-HAR (**21**) (m/z): $[\text{M}+\text{H}]^+$ calcd. for $\text{C}_{15}\text{H}_{30}\text{NO}_6$ 320.2068; found 320.2050.

Synchronized worm cultures for comparative metabolomics of the exometabolome

For making synchronized adult cultures, 40 L4 worms were placed onto a 10 cm NGM agar plate seeded with 25X HB101 bacteria. After 96–100 h at 22.5 °C, the worms were washed from the plate using 0.1 M NaCl and transferred to a 50 mL tube. The worms were washed three times with 0.1 M NaCl, bleached using 2.5 mL H_2O , 2.5 mL 10 M NaOH, and 2.5 mL sodium hypochlorite (Sigma 425044). The eggs were allowed to hatch in 5 mL M9 buffer for 24 h. The next day, about 6000 L1 worms/plate were placed onto three 10 cm NGM agar plates, each seeded with 25X HB101. After about 2.5 d at 22.5 °C, the worms from all the plates were combined by washing, and the eggs were obtained by bleaching. After 24 h, the liquid culture was started by inoculating about 200,000 synchronized starved L1 worms into 25 mL of S medium in a 250 mL Erlenmeyer flask supplemented with 2% (w/v) 25X HB101. The worms were grown in a shaker at 22.5 °C at 220 rpm, and food was added every 24 h. After 60 h, 20 mL of growth medium was collected, freeze-dried, and stored at -20 °C until further use. To extract, 20 mL of methanol was added to the dried medium and extracted overnight in a rotating shaker at 150 rpm. The extracts were filtered through a small plug of cotton in a pasteur pipette and dried in a rotary evaporator. Dried concentrated extracts were resuspended in 120 μ L of 50% methanol in water for LC-HR-MS/MS. All the experiments were performed in biological triplicate.

LC-HR-MS/MS analysis

All LC-HR-MS/MS was performed on a Bruker Impact II QTOF mass spectrometer coupled with an UltiMate 3000 RSLC nano System using a previously described method with the following chromatographic changes.⁵² Samples were separated on a Hypersil GOLD aQ Polar Endcapped C18 3 μ m 175 \AA (2.1 x 150 mm) column using 10 mM ammonium formate with 0.1% formic acid as mobile phase A and acetonitrile with 0.1% formic acid as mobile phase B. The LC-MS gradient was started with 5% B for 5 min and then linearly increased up to 99% at 25 min and then held constant for 7 min. All the samples were analyzed in positive and negative ESI mode. For MS/MS analysis, we acquired all the data in data dependent acquisition mode where the mass spectrometer selected the top 3 most intense precursor ions at the first stage for further fragmentation. An active exclusion window of 3 precursor ions for 1 min was selected which prevented repeated fragmentation of the same precursor ions and allowed less abundant ions to fragment. A minimum intensity target of 10,000 counts was selected for MS/MS data acquisition. The mass spectrometry parameters were set as following: end plate offset 500 V, capillary voltage 2.5 kV, collision RF 2500 Vpp, transfer time 50.0 μ s, prepulse storage 5 μ s, collision energy 25.0 eV. A mass range of m/z 50–1300 was used.

Processing of comparative metabolomics data

For all data processing steps and feature detection, Metaboscape (version 5.0) software platform (Bruker) was used. To extract differential features from the datasets, the raw data files of biological triplicate samples from control and mutant groups were uploaded onto Metaboscape, and peaks were selected with a signal intensity greater than 1×10^3 counts and with a mass range of m/z 150–1500. A t-test was performed to generate a volcano plot with differential features. If not combined automatically, significant features with multiple adduct ions were manually combined.

Purification and structure elucidation of asc-C6-pip (**29**)

A total of 18 L of mixed-stage wild-type worm culture was grown. 600,000 to 800,000 worms were added per liter of S medium in 2.8 L baffled flasks and shaken for 10 d at 215 rpm at 22 °C. 20 mL of 25X HB101 bacteria in S medium was added every day to each 1 L of worm culture. After 10 d, the culture was centrifuged at 2,675 g for 10 min, and the medium was collected and stored frozen at -20 °C. The frozen medium was lyophilized and then extracted with 190-proof ethanol using a volume equal to the original medium (shaking at 200 rpm for 12 h). The ethanol was evaporated using a rotary evaporator, and the extract was dissolved in about 30 mL of 10% methanol, subjected to C18 column chromatography (46 mm x 300 mm), and eluted with a stepwise gradient of 10%, 20%, 30%, 40%, 60%, 80%, and 100% (v/v) methanol in water (500 mL for each fraction) to obtain 7 fractions. The third fraction contained the majority of asc-C6-pip (**29**) by LC-MS and was subjected to silica gel chromatography (25 mm x 500 mm) and eluted with CH_2Cl_2 :methanol (30:1 to 0:1) to obtain 16 fractions. The seventh and eighth fractions were combined and subjected to Sephadex LH-20 chromatography (30 mm x 1050 mm) using methanol as a solvent to obtain approximately 2.5 mg of semi-pure asc-C6-pip (**29**) as a white oil; NMR data are in Table S1; HR-ESIMS (m/z): $[\text{M}+\text{H}]^+$ calcd. for 330.2275, found, 330.2276.

Dauer formation

The ascariosides (1 μ M in ethanol) were added to NGM agar (without peptone and cholesterol) in a 3.5 cm plate. Subsequently, heat-inactivated OP50 (8 mg/mL) was added to the plate. A few young adults were placed on the plate for 2 h at room temperature to lay 60–100 eggs. The young adults were removed, and the plate was incubated for 2 d at 25 °C before scoring for dauers. All experiments were carried out in triplicate, and two independent experiments were performed with similar results.

Lifespan assay

Synchronized L1s were transferred to 6 cm NGM agar (without peptone) plates containing 25 μ M 2'-deoxy-5'-fluorouridine (FUdR) and seeded with 200 μ L of 25X OP50 containing 25 μ M FUdR, and the L1s were allowed to grow to the adult stage. Meanwhile, assay plates were made by adding vehicle (ethanol) or 125 nM asc-C6-pip (**29**) to warm NGM agar (without peptone) containing 25 μ M FUdR before adding the NGM-agar to 6 cm plates to solidify. The assay plates were seeded with 200 μ L of 25X bacterial OP50 containing 25 μ M FUdR. Once the worms reached adulthood, 30 worms were transferred to the assay plates. The survival of the worms was monitored daily. The worms were considered dead if they did not respond to a gentle tap from a platinum pick and did not have pharyngeal pumping. Any worms that died by crawling up the side of the plates were censored. All experiments were carried out in triplicate, and two independent experiments were performed with similar results.

Chemotaxis assay

The chemotaxis assay was adapted from a previously published protocol.⁵³ The vehicle (ethanol) and test sample were placed 4 cm apart on a 6 cm NGM agar (without peptone) plate, followed by addition of 1 μ L of 1M sodium azide. Once the samples were dried, wild-type young adult hermaphrodites or males were placed equidistant between the vehicle (dimethyl sulfoxide) and test sample. The young adult hermaphrodites were produced from synchronized L1s placed on 10 cm NGM agar plates seeded with 750 μ L of 25X OP50 at 25 °C for 2 d, and then the young adults were washed twice with M9 buffer prior to the assay. The young adult male worms were generated through mating, picked to a new NGM agar plate without bacteria, and washed twice with M9 buffer prior to the assay. After 2 h, any worms within a 0.5 cm radius of either test spot were counted. The chemotaxis index was calculated using the chemotaxis index equation: (number of worms at test sample – number of worms at control) divided by (total number of worms on the agar plate). A positive chemotaxis index indicates attraction, while negative chemotaxis index indicates avoidance. The experiment was performed in triplicate, and three independent experiments were performed with similar results.

Ascaroside analysis for worm cultures supplemented with different amino acids

Wild-type worms were grown on a 10 cm NGM agar plate, spotted with 800 μ L 25X HB101, at room temperature until the bacteria were almost consumed. The plate was washed with 10 mL of S medium, which was added to 140 mL of S medium in a 500 mL flask. The worms were grown at 22.5 °C for 5 d and fed with 3 mL of 25X HB101 every day. Around 8000 mix-stage wild-type worms were transferred to 5 mL of S medium in a 50 mL centrifuge tube (day 1). The worms were grown at 22.5°C for 7 d and fed with 300 μ L of the following food stocks: 4.5 mL of 25X HB101 mixed with 0.5 mL of water (control) or 100 mM Gln, Glu, Asp, Pro, or Lys. For sample collection, the culture was incubated in an ice-bath for 30 min to 1 h to settle the worms, and the supernatant was centrifuged (800 g for 5 min). 4 mL of supernatant was loaded onto a 200 mg C18 Sep-Pak column (Waters), which was washed with water (3 mL) and eluted with methanol (3 mL). The methanol elution was dried by SpeedVac and resuspended in 100 μ L of 50% (v/v) ethanol in water, and the ascarosides were analyzed by LC-MS.

Preparation of bacterial powder

An OP50 colony was used to inoculate a 5 mL culture in Luria-Bertani (LB) medium and incubated with shaking at 37 °C for 6-8 h. This 5 mL culture was used to inoculate a 1 L LB culture, shaking at 37 °C overnight. The OP50 was collected in autoclaved centrifuge bottles by centrifuging at 2,675 g for 10 min and discarding the supernatant. The OP50 pellet was resuspended in 40 mL of autoclaved water. This 25X bacterial stock was then disrupted using a Sonic Dismembrator Model 500. Disruption was performed with 5 cycles at 70% amplitude, each cycle consists of 7 pulses for 10 s with a 60 s delay between each pulse. Disrupted cells were frozen at –80 °C and lyophilized until completely dry. The bacterial powder was dissolved in sterile water to achieve a 60 mg/mL concentration and plated to ensure that no colonies grow.

Ascaroside analysis for worm cultures supplemented with labeled lysine

Approximately 15,000 arrested wild-type L1 larvae obtained from alkaline bleach treatment were added to a 50 mL tube containing 5 mL of S medium with 2 mM lysine-HCl or lysine-*d*₄-HCl (C/D/N Isotopes, D-2554). Worms were fed with 15 mg of bacterial powder. Worms were incubated at 22.5°C with shaking at 200 rpm for 72 h, at which time the population was a mixture of young and gravid adults, as determined by microscopic inspection. Cultures were centrifuged at 800 \times g for 5 min, and the resulting supernatant was frozen at –80°C for 1 d. Frozen medium was lyophilized and extracted with 5 mL of methanol. Extracts were dried by SpeedVac, resuspended in 50% (v/v) ethanol in water, and analyzed by LC-MS. For culturing arrested L1 larvae in the absence of any food, approximately 20,000 wild-type eggs obtained from alkaline bleach treatment were added to a 50 mL tube containing 5 mL of M9 medium with 2mM lysine-HCl or lysine-*d*₄-HCl (C/D/N Isotopes, D-2554). Eggs were allowed to hatch and develop into arrested L1 larvae by incubating at 22.5°C with shaking at 200 rpm for 48 h. Cultures were centrifuged at 800 \times g for 5 min, and the resulting supernatant was frozen at –80 °C for 1 d. Frozen medium was lyophilized and extracted with 5 mL of methanol. Extracts were dried by SpeedVac, resuspended in 50% (v/v) ethanol in water, and analyzed by LC-MS.

Ascaroside analysis for worms grown on bacterial mutant strains

Wild-type worms or mutant worms for candidate genes in the 1-piperidine pathway were grown on 6 cm NGM agar plates at room temperature until the bacteria (25X, 200 μ L) on the plate were almost consumed. The plate was washed with 5 mL of S medium and transferred to a 50 mL tube (day 1). The worms were grown at 22.5 °C for 5 d and were fed with 500 μ L of 25X OP50,

BW25113 (wild-type), JW0181 (*ldcC*), JW4092 (*cadA*), or JW5510 (*patA*) every day. For sample collection in these experiments, the culture was chilled in an ice-bath for 30 min to 1 h to settle the worms, and the supernatant was centrifuged (800 g for 5 min). 4 mL of supernatant was loaded onto a 200 mg C18 Sep-Pak (Waters) column, which was washed with water (3 mL) and then eluted with methanol (3 mL). The methanol fraction was dried by SpeedVac and resuspended in 100 μ L of 50% (*v/v*) ethanol in water, and the ascarosides were analyzed by LC-MS.

Ascaroside analysis for worms grown on *C. elegans* microbiome strains

The worms were synchronized by alkaline bleach treatment followed by allowing the L1 worms to arrest in M9 buffer for 24 h. The arrested L1 worms were seeded onto 10 cm plates containing 750 μ L 25X OP50 for 52 h. After 52 h, the eggs were harvested from the gravid adults by alkaline bleach treatment. Approximately 25,000 arrested L1 worms were added to 5 mL of S medium and fed with 1 mL of 25X of either OP50, HB101, or selected microbiome strains (BIGb0170, Jub44, MYb10, MYb11, and BIGb0393) at 0 h, 24 h, and 48 h. The culture medium was harvested when worms reached the gravid young adult stage. The majority of worms fed on different bacterial strains reached the young adult stage in 55–60 h, but worms grown on BIGb0170 required 75 h to reach the young adult stage. The cultures were centrifuged at 2,675 g to remove worms and bacteria, and the culture mediums were frozen at -80°C , lyophilized, and extracted using 5 mL of methanol for 16 h. The extracts were dried by SpeedVac and resuspended with 120 μ L of 50% (*v/v*) methanol for LC-MS analysis.

QUANTIFICATION AND STATISTICAL ANALYSIS

All error bars represent the mean \pm standard deviation, and *p* values were calculated using either an unpaired *t* test or one-way ANOVA using GraphPad Prism. The lifespan assays were analyzed using Kaplan-Meier survival curves that were compared using a log-rank test in GraphPad Prism. Dauer formation, lifespan, and chemotaxis assays were performed in triplicate and were repeated at least once in a biologically independent experiment to confirm results.